Arc-Continent Collisions, Sediment Recycling and the Maintenance of the Continental Crust

PETER CLIFT

School of Geosciences, University of Aberdeen, Meston Building, Kings College, Aberdeen, AB24 3UE, United Kingdom, and DFG-Research Centre Ocean Margins (RCOM), Universität Bremen, Klagenfurter Strasse, 28359 Bremen, Germany

HANS SCHOUTEN

Department of Geology and Geophysics, Woods Hole Oceanographic Institution, Woods Hole MA 02543, USA

PAOLA VANNUCCHI

Dipartimento di Scienze della Terra, Università deli Studi di Firenze, Via La Pira, 4, 50121 Firenze, Italy

Abstract: Subduction zones are both the source of most new continental crust and the locations where crustal material is returned to the upper mantle. Globally the total amount of continental crust and sediment subducted below forearcs currently lies close to 3.0 Armstrong Units (1 AU = 1 km^3/yr), of which 1.65 AU comprises subducted sediments and 1.33 AU tectonically eroded forearc crust. This compares with average ~0.4 AU lost during subduction of passive margins during Cenozoic continental collision. Individual margins may retreat in a wholesale, steady-state mode, or in a slower way involving the trenchward erosion of the forearc coupled with landward underplating, such as seen in the central and northern Andean margins. Tephra records of magmatism evolution from Central America indicate pulses of recycling through the roots of the arc. While this arc is in a state of long-term mass loss this is achieved in a discontinuous fashion via periods of slow tectonic erosion and even sediment accretion interrupted by catastrophic erosion events, likely caused by seamount subduction. Crustal losses into subduction zones must be balanced by arc magmatism and we estimate global average melt production rates to be 96 and 64 km^3/m.y./km in oceanic and continental arc respectively. Key to maintaining the volume of the continental crust is the accretion of oceanic arcs to continental passive margins. Mass balancing across the Taiwan collision zones suggests that almost 90% of the colliding Luzon Arc crust is accreted to the margin of Asia in that region. Rates of exhumation and sediment recycling indicate the complete accretion process spans only 6–8 m.y. Subduction of sediment in both erosive and inefficient accretionary margins provides a mechanism for returning continental crust to the upper mantle. Sea level governs rates of continental erosion and thus sediment delivery to trenches, which in turn controls crustal thicknesses over 10^7–10^9 yrs. Tectonically thickened crust is reduced to normal values (35–38 km) over timescales of 100–200 Ma.

Introduction

The origins of the continental crust and the timing of its generation have been contentious issues in the Earth sciences for many years, largely revolving around arguments about whether the vast majority of the crust was generated during the Archaean (Armstrong & Harmon 1981; Bowring & Housh 1995; Elliott *et al.* 1999; Goldstein *et al.* 1997), or whether growth has been more gradual since that time (Albarede & Brouxel 1987; Ellam &

Hawkesworth 1988; Moorbath 1978; O'Nions *et al.* 1979). More recently it has been suggested that continental crust has largely been generated in a series of rapid bursts of production between 1 and 3 Ga that were linked to rapid convection events in the mantle (Hawkesworth & Kemp 2006). In this model new upper crust is formed by differentiation from melt, leaving a large volume of dense residue, which may then be recycled back into the upper mantle via gravitational delamination. Generation of significant volumes of new crust does not appear to have been associated with areas of greatly thickened continental crust.

Although such an explanation implies that mantle plumes may have been fundamental in the generation of some early crust (e.g., West African and Arabian Shields (Boher *et al.* 1992; Stein & Hofmann 1994)), most geochemical evidence instead indicates that subduction magmatism was the dominant source of new crustal material, especially during the Phanerozoic. Although continental crust is generally more andesitic than most modern arc magmatism (Rudnick 1995), a combination of geochemical and tectonic evidence indicates that active margins are likely the principle source of the continental crust (Barth *et al.* 2000; Dewey & Windley 1981; Rudnick & Fountain 1995; Taylor & McLennan 1995). Exactly how new crust is generated and how rapidly this is recycled through the subduction zones is however still enigmatic. In this paper we examine the rates of mass recycling through subduction zones and assess the role of oceanic arc accretion in building and maintaining the continental crust. We specifically focus on the Phanerozoic when tectonic processes were the same as in modern plate tectonics. In this respect we do not try to understand how crust is recycled on the gigayear timescale, but rather how the volume of continental crust is maintained in the present tectonic regime. We do this by generating mass budgets for sediment and crustal flux to the global trench systems and comparing this with other possible mechanisms for crustal loss.

Generation of the continental crust in the first place is only part of the process of how the modern continents were formed and is not the focus of this paper, which is the role that subduction processes play in the maintenance of the crust during Phanerozoic times. Some constraints on long-term crustal volumes have been gained through consideration of variations in global sea level. Because the volume of the ocean basins is controlled by the relative proportions of continental versus oceanic crust a progressive loss or gain of continental crust would necessarily result in long-term variations in the global sea level, assuming that the volume of water on the Earth's surface has remained roughly constant. Although sea level has varied in the geological past, the magnitude of the change over a variety of timescales is modest compared to the total depth of the ocean basins (~200 m compared to mostly 3–6 km; (Haq *et al.* 1987)) and there has been little net change since at least the start of the Phanerozoic. Schubert & Reymer (1985) argued that because of the generally constant degree of continental freeboard (i.e., the average height of the continents above sea level) since the Precambrian, the continental crust must have remained close to constant volume since that time. In fact these authors argued that gradual cooling of the Earth has resulted in slight deepening of the ocean basins, implying slow crustal growth since that time. This slow growth model is supported by Nd isotopic evidence for continental extraction from the upper mantle (Jacobsen 1988), as well as new Hf-O oxygen isotope data from zircons in cratonic rocks (Hawkesworth & Kemp 2006). Thus there appears to be a long-term balance between growth of new continental crust through arc magmatism and recycling of this crust back into the mantle via subduction zones.

Mass Budgets for the Continental Crust

Subduction of Continental Crust

For many years it was believed that large-scale subduction of continental material was impossible because of the density differences between continental crust, oceanic crust and the upper mantle. Nonetheless, if continental crust is generated at convergent margins then this requires some type of return flow to the upper mantle for the volume balance inferred from the freeboard argument to be maintained. While some have argued for delamination and loss of lower crustal blocks (Gao *et al.* 2004), others have suggested that large volumes of crust can be subducted during major collisional orogens (Hildebrand & Bowring 1999; Johnson 2002).

An estimate of the degree of crustal recycling possible during continental collisions can be derived by considering the Earth's mountain belts formed by continent-continent and arc-continent (passive margin) collisions during the Cenozoic. In practice this means the Neotethyan belts of the Mediterranean, the Middle East and Himalayas, as well as Taiwan and the Ryukyu Arc, northern Borneo and the Australia-Papua New Guinea region. In total these sum to almost 16,000 km of margin (Table 1). We assume a gradual thinning of the crust across these margins due to the progressive extension prior to break-up, and thus an average crustal thickness of 18 km (half normal continental (Christensen & Mooney 1995)). We further assume that like the modern oceans around 50% of the subducted margins were volcanic (50 km wide continent-ocean transition (COT)) and the remainder non-volcanic (150 km wide COT). The sedimentary cover to colliding margins is usually imbricated into the orogen but apart of small occurrences of high-grade rock subducted and then re-exhumed to the surface (e.g., (Leech & Stockli 2000; Ratschbacher *et al.* 2000) the crystalline crust is potentially lost to the mantle. We calculate that around 28 x 10^6 km^3 have been subducted since the Mesozoic, resulting in a long-term average of 0.43 Armstrong Units (1 AU = 1

km^3/yr). Table 1 shows the basis of this estimate, involving the subduction of around 2.8 x 10^9 km^3 of passive margin crust since 65 Ma. If we assume that all the subducted margins were non-volcanic then the total subducted would increase to 4.2 x 10^9 km^3 and the long-term recycling rate to 0.65 AU.

Mechanisms of Subduction Erosion

This study focuses on quantifying the processes by which crust is returned to the mantle via subduction zones. von Huene & Scholl (1991) synthesized a series of earlier studies and proposed that large volumes of sediment and forearc crust, are being subducted in modern trenches. The concept that convergent margins not only accrete trench sediments in forearc prisms (accretionary wedges) but also allow deep subduction of continental material within a "subduction channel" was pioneering. Tectonic erosion of some plate margins had been recognized before (Hilde 1983; Miller 1970; Murauchi 1971; Scholl *et al.* 1977), but von Huene & Scholl (1991)'s idea that this was a process common in many of the Earth's subduction zones helped geologists reconcile the apparent mis-match between a stable crustal volume and the ongoing arc magmatism. Their study helped properly establish the fact that there are two end member types of active margin, accretionary and erosive, and that the latter are common, especially in the Circum-Pacific region (Figs. 1 and 2).

It is still not yet agreed quite how tectonic erosion is accomplished, with competing models suggesting mechanical abrasion by fault blocks on the underside of the subducting plate acting like a "buzz saw" (Hilde 1983), while others emphasize the importance of subducting aseismic ridges in abrading material from the forearc (Clift & MacLeod 1999; Clift *et al.* 2003a; Ranero & von Huene 2000; Vannucchi *et al.* 2003; von Huene & Ranero 2003). Alternatively, the importance of fluids in this process was first suggested by von

Huene & Lee (1982). In this type of model water expelled from the subducting plate causes hydrofracturing and disintegration of the base of the overlying forearc (Platt 1986; von Huene *et al.* 2004). The disrupted fragments would then be released into the subduction channel and transported to depth, either to the roots of the volcanic arc or even to the upper mantle. Evidence from the first recognized palaeo-subduction channel in the Italian Apennines shows that material was being returned to the deep Earth via a 500-m-wide zone and that tectonic erosion of the forearc wedge was occurring both on its underside and frontal "toe" region (Vannucchi *et al.* 2008).

Clift & Vannucchi (2004) used large-scale, long duration (>10 m.y.) estimates of forearc mass change to improve the estimated rates of accretion or mass loss in all convergent margins. They predicted that around 3.6 AU were being subducted globally, rather higher than the 1.6 AU estimated by von Huene & Scholl (1991). They recorded 57% of modern trenches as being in a long-term tectonically erosive mode (Fig. 1) and noted that there was a correlation between margins where there was less than 1 km of sediment in the trench and tectonic erosion. In contrast, margins with >1 km of trench sediment were sites of net accretion (Fig. 3). Because the last 2–4 m.y. are generally recognized as being a period of faster than normal continental surface erosion (Zhang *et al.* 2001), and presumably faster clastic trench sedimentation, it seems likely that 1 km is an over-estimate of this threshold over long periods of geologic time. This is because the Plio-Pleistocene pulse of faster sediment supply would not have had sufficient time to impact the long term growth rates of convergent margins. 400 m is however an absolute lower bound to the accretionary threshold because this is the thickness of purely pelagic sediment found in many trenches in both the eastern and western Pacific Ocean, where there are no clastic trench sediments and where long-term tectonic erosion is recorded. Because of the increased superficial erosion linked to glacial cycles the Earth's subduction systems are likely to now be in a particularly accretionary mode, and that prior to Northern Hemispheric Glaciation tectonic erosion would have been even more dominant.

An important feature of accretionary margins is that while they are regions of net continental growth this does not mean that no continental crust is being recycled to the mantle in these margins (von Huene & Scholl 1991). Indeed, over long periods of geologic time the proportion of sediment reaching the trench and preserved in accretionary margins averages only ~19% globally (Clift & Vannucchi 2004). It is not clear whether this is because subduction accretion is a very inefficient process, or because even accretionary margins suffer phases of tectonic erosion, perhaps triggered by subduction of seamounts or aseismic ridges. Drilling and modelling of the accretionary wedge in the Nankai Trough of SW Japan indicates that décollement in the trench sediment pile preferentially occurs near the base of the coarser grained trench sands, while the finer grained hemipelagic sediments below seem to be underthrusted, at least below the toe region of the wedge (Le Pichon *et al.* 1993). This means that a significant proportion of the trench sediment column is underthrust at that, and presumably most other margins, even when no ridge or seamount collision is occurring. Mass loss rates increase during subduction of aseismic ridges. 3D seismic reflection data has shown that such ridges have resulted in temporary periods of tectonic erosion, followed by a reversion to more efficient sediment accretion (Bangs *et al.* 2006).

Non-Steady State Tectonic Erosion

Observations of shallow water or subaerial sedimentary rocks now found in trenches indicate long-term crustal loss over periods of $>10^7$ yr, but do not preclude shorter intervals of net accretion. Conversely margins in a state of long-term net accretion may also experience periods of tectonic erosion, usually linked to the passage of seamounts or other topographic features on the subducting plate. Some estimates of the time scale of these alternations can be derived from reconstructions of vertical tectonic motions. Melnick & Echtler (2006) used seismic data from the southern Andean margin to show that the marine forearc in this area has experienced basin inversion and uplift since the Pliocene, reversing a long-term trend to subsidence and crustal loss. In that study inversion was attributed to the increased sediment flux to the trench due to faster continental erosion driven by the glacial-interglacial cycles. Increased sediment flux was inferred to lubricate the base of the forearc wedge, reducing friction along that contact and driving a readjustment of the critical angle of the wedge. In this respect the model followed the suggestion by Lamb & Davis (2003) that reduced sediment flux to the central Andean trench increased coupling between over-riding and subducting plates and triggered uplift of the main Andean ranges. If this were true then the total crustal flux to the upper mantle would increase as continental erosion increased.

Further north variability in the flux of material through the subduction zone is better constrained thanks to linked onshore-offshore data sets. The Andean margin of Peru and northern Chile provides a good example of an active margin in a state of long-term mass loss (von Huene & Ranero 2003). About 250 km of crust is estimated to have been lost from the western edge of South America in northern Chile and southern Peru since 150 Ma (Rutland 1971; Scheuber & Reutter 1992; Stern 2004), with as much as 30 km of this loss occurring since 10 Ma (Laursen *et al.* 2002). A landward step of 30–40 km in the trench axis north of the Juan Fernandez Ridge since 10 Ma resulted in trench retreat rate estimates of about 3.0 km/m.y. during the Miocene-Recent, with similar values estimated from offshore Mejillones (von Huene & Ranero 2003). In such an environment forearc subsidence is predicted and has been observed in seismic and drilling data (Clift *et al.* 2003a; Laursen *et al.* 2002; von Huene & Ranero 2003)(Fig. 4), with temporary periods of uplift at the point where aseismic ridges are in collision with the trench.

Comparison of onshore and offshore data in the central Andes however indicates that the margin is not in a continuous state of wholesale landward retreat. Sedimentary evidence from basins exposed along the coast demonstrates that the shoreline has been relatively stationary since 16 Ma and has not migrated inshore, as might be expected. Moreover, the exposure of these basins and the presence of marine terraces over long stretches of the margin (Fig. 5) point to recent uplift since at least the start of the Pleistocene (~1.8 Ma). Subsidence analysis backstripping methods were applied by Clift & Hartley (2007) to measured sections from these onshore coastal basins in order to isolate the tectonically driven subsidence of the basement, after correcting for sediment loading and sea-level variability. Although rates of tectonic erosion and subsidence are much higher close to the trench the continental basins are useful because the shallow shelf depths involved provide relatively high precision constraints on vertical motions compared to deep-water trench or slope sediments.

Figure 6 shows the results of these analyses for the Pisco, Salinas, Mejillones, Caldera and Carrizalillo Basins. What is remarkable is that all these basins show a coherent, albeit slow basement subsidence, as might be predicted for a tectonically erosive margin, since 16 Ma, at the same time as the trench is known to retreat landwards and the marine forearc to subside (Fig. 4). However, like the southern Andean basins (Melnick & Echtler 2006) they also all show a late Pliocene unconformity, followed by terrestrial and coastal sedimentation preserved in a series of Pleistocene terraces. Although uplift can be generated by flexure in the footwall of normal faults, this is necessarily localized. However, the regional style of uplift observed along long stretches of the Andean coast and in the form of extensive terracing across a zone 5–10 km wide requires regional crustal thickening. This is most likely caused by subduction accretion and basal underplating of the forearc crust. The observation of active extensional faulting in much of the forearc precludes thickening by horizontal compression and thrust faulting. The central Andean margin experiences tectonic erosion but instead of the wholesale retreat of the plate margin the forearc is constrained to steepen since 16 Ma (Fig. 7A) and then experience underplating since 2 Ma. As a result mass flow rates are much lower here than would be predicted for a steady-state erosive margin.

It is tempting to relate the Pleistocene shift to limited accretion under much of the terrestrial forearc due faster trench sedimentation forced by climatic changes during the onset of Northern Hemispheric glaciation, much, as suggested for the southern Andes (Melnick & Echtler 2006). However, this model does not hold up in the central Andes where there are effectively no trench clastic sediments even today, reflecting the very arid climate of the continental interior. We conclude that the recent change in trench tectonics in the Andes is likely driven by a tectonic change in the way that the Pacific and South American plates interact.

Analysis of seismic and drilling data from the Andean forearc offshore the Lima Basin (Figs. 4 and 5) also suggests that tectonic erosion is a temporally and spatially discontinuous process. Backstripping analysis of Ocean Drilling Program (ODP) Site 682 on the trench slope has been used to demonstrate long-term mass loss (Fig. 6)(Clift *et al.* 2003a), accelerating after the collision of that part of the trench with the aseismic Nazca Ridge. Like the onshore basins to the south ODP Site 679, also located in the Lima Basin but in shelf water depths, shows slow basement subsidence, with temporary uplift during passage of the Nazca Ridge along this part of the trench at 11–4 Ma (Fig. 5)(Hampel 2002). However, interpretation of seismic lines across the forearc (Clift *et al.* 2003a)(Fig. 4) shows that the trenchward part of Lima Basin has been uplifted >500 m relative to the landward portions of the basin since the end of the Pliocene. This suggests Pleistocene underplating of the outer part of the forearc, where typically subduction erosion is most rapid. Uplift is consistent with the observation of a small accretionary complex at the foot of the trench slope in this region (Fig. 4A). The Aleutian forearc provides an additional example of this kind of process because although a significant accretionary wedge is developed at the trench the mid forearc is dominated by a deep basin whose subsidence can only be explained by major basal erosion of the wedge (Ryan & Scholl 1993; Wells *et al.* 2003). Clearly accretion and erosion are spatially and temporally variable, even on a single length of margin.

Geochemical Evidence for Temporal Variations

Changes in the rates of sediment subduction and forearc tectonic erosion affect forearc vertical motions but must also impact the chemistry of arc volcanism. Geochemical evidence exists in Central America to suggest variations on the 1–4 m.y. timescale in tectonic erosion, as well as related but independent changes in sediment subduction. In Costa Rica two different views of mass flux have been proposed. Tectonicists have shown that the margin and trench slope are in a state of long-term subsidence and presumed mass loss due to subduction erosion (Meschede *et al.* 1999; Vannucchi *et al.* 2001; Vannucchi *et al.* 2003). Geochemical data from the active arc (e.g., ^{10}Be isotopes) indicates that the sedimentary cover in the modern trench cannot presently be contributing significantly to petrogenesis. This has been interpreted to imply that either the sediment is being off-scraped and accreted to the margin (Morris *et al.* 2002; Valentine *et al.* 1997), or that tectonic subduction erosion is adding large volumes of additional material to the subduction channel so that the sedimentary signal to the arc magma is strongly diluted (Vannucchi *et al.* 2003). Early geophysical surveys had proposed that the Costa Rican forearc was largely comprised of an accretionary wedge (Shipley *et al.* 1992), yet drilling of the region by ODP Leg 170 demonstrated that in fact the slope was formed by an extension of the onshore igneous Nicoya Complex, mantled by a relatively thin sedimentary apron of mass wasted continental detritus and hemipelagic sediments (Kimura *et al.* 1997). Although the ODP drilling ruled out the possibility of much accretion of oceanic sediments at the toe of the forearc wedge during the recent geologic past, drilling was not able to show whether sediments have been transferred to the overriding plate by underplating at greater depths. Clearly competing models advocating accretion and erosion cannot both be correct, at least over the same time scales.

Study of the tephras deposited offshore the Nicoya Peninsula, Costa Rica, offer a possible explanation to these contradictory lines of evidence. Tephras can be used to reconstruct the magmatic evolution of the adjacent arc (the prevailing winds blow directly offshore) because the isotopic composition of the arc magmas (from which the tephras are derived) reflects the degree of sediment and forearc recycling in the subduction zone. As a result the isotope geochemistry of the tephras can be used to quantify the degree of recycling at the time of their deposition. The cause of the tectonic erosion cannot be constrained from the tephras alone, but is inferred in this case from modern geophysical data that indicate this process to be the primary cause of erosion in Costa Rica (Ranero & von Huene 2000).

Tephra glasses younger than 2.5 Ma were analyzed by microprobe and found to be essentially unaltered, allowing them to be used to trace the temporal evolution of the onshore volcanic arc (Clift *et al.* 2005a). Trace element characteristics were compared to the active arc and a generally good fit was recognized between the tephra and the Costa Rican part of the central American volcanic zone, a match that is possible because of the major along strike variability noted between Costa Rica, Guatemala and Nicaragua (Carr *et al.* 2003; Leeman *et al.* 1994; Patino *et al.* 2000; Reagan *et al.* 1994). Clift *et al.* (2005a) employed Li and Nd isotopes to quantify the influence of sediment subduction and tectonic erosion on arc petrogenesis, an approach that was possible because of the different isotopic characteristics of trench sediments, the Nicoya Complex forearc basement and the altered oceanic crust entering the trench (Fig. 8A). These end members allow the relative contributions of these sources to be resolved and unmixed. Figure 8B shows that at 1.45 Ma an unusual tephra was deposited showing an anomalous composition in Nd isotopes (i.e., relatively negative ε_{Nd}). This composition departs sharply from that of the nearest Costa Rican arc volcano, Arenal, as well as the other tephra in the stratigraphy, thus indicating a short-lived pulse of enhanced continental sediment subduction. The Li isotope composition also shows strong temporal variability, with high δ^7Li values being achieved at and for around 0.5 m.y. after the ε_{Nd} spike. Subsequently δ^7Li reduced to low values at the present day. These trends were interpreted to show that both sediment subduction and forearc erosion are currently at low levels, as inferred from study of the volcanoes themselves, but that this pattern is atypical of the recent geologic past. The patterns of isotope evolution may reflect collision of a seamount with the trench before 1.45 Ma, driving subduction of a sediment wedge formed there, and subsequently increasing erosion and subduction of forearc materials. The whole cycle from accretion to erosion and back to accretion appears to span <2 m.y.

Rates of Mass Recycling

Rates of Sediment and Crustal Subduction

Table 2 presents revised estimates of the rates of sediment accretion, tectonic erosion and arc magmatism for global active margins based on the study of Clift & Vannucchi (2004), but updated with new constraints for some crucial margins. These figures indicate less crustal subduction than proposed in the earlier study, mostly as a result of reduced estimates for tectonic erosion in the Andean margin of Peru and northern Chile (Clift & Hartley 2007). Even so, we estimate that worldwide total continental mass subduction lies close to 3.0 AU, compared to around 3.6 AU in the synthesis of Clift & Vannucchi (2004), but still more than the 1.6 AU of von Huene & Scholl (1991). This value is almost an order of magnitude more than the 0.4 AU estimate for recycling of subducted passive margins in orogenic belts (Table 3).

The total amount of sediment being subducted at the world's trenches is relatively well constrained, because trench sediment thicknesses and convergence rates are relatively well known. In contrast, rates of subduction erosion of forearc crust are less well documented and appear to be quite variable in time. Of the total continental crust subducted globally at least as deeply as the magmatic roots of the arc systems we estimate that 1.65 AU comprise subducted sediments, with 1.33 AU of eroded forearc. Thus the latitude for error in the total estimate principally lies in the 1.33 AU of tectonic erosion. Regions where this value is not well known are themselves becoming scarcer. While the degree of tectonic erosion may change due to further research we believe that the amount of change in the total sum cannot be too large and that the 3.0 AU recycling rate is unlikely to be more than ~20% in error.

Rates of trench retreat are the most common source of tectonic erosion estimates and many are based on the identification of terrestrial or shallow-water sediments overlying basement on the trench slope of modern systems (Clift & MacLeod 1999; Laursen *et al.* 2002; Vannucchi *et al.* 2001; Vannucchi *et al.* 2003; Vannucchi *et al.* 2004; von Huene *et al.*

1982). Rates of loss are then calculated based on the distance between the modern location of the shallow water sedimentary rock and the location where similar facies sediments are now being deposited in the modern forearc. Rates of trench retreat are then derived by dividing this across-strike distance by the age of the sedimentary rock. Trench retreat rates in turn can be converted to rates of crustal volume loss if the thickness of the forearc crust is known and if the mode of subduction erosion is assumed. In the simplest and most conservative model trench retreat occurs along a margin in which the geometry remains effectively constant through time. Figure 7B shows that in this case a retreat of any given distance must involve loss of a complete crustal section of this width, since the forearc wedge itself remains constant. However, over short time spans tectonic erosion can result in steepening of the forearc slope and a retreat of the trench with much lower total volumes of crustal subduction (Clift & Hartley 2007).

Rates of Arc Magmatism

Although short-term variations in mass flux through any given subduction zone can be driven by ridge and seamount collisions, or even climatically induced changes in trench sedimentation the recognition that some margins have been in a long-term state of erosion or accretion allows mass budgets for plate margins to be made over periods of geologic time 10^7 yr or longer. As argued above, this loss has been balanced by arc magmatism, assuming a relatively constant volume of water at the Earth's surface and in the presence of a stable sea level. Although Clift & Vannucchi (2004) calculated that this rate of production averaged ~90 km^3/m.y./km of trench this figure can now be reduced in light of the much lower crustal recycling rates for the Central and Northern Andes (Clift & Hartley 2007). Because of the length of the Andean margin and the thickness of the continental crust here this adjustment makes a significant difference to the rate of loss and brings the global average rate of arc production down to 74 km^3/m.y./km. The rate of recycling is likely to change as more geophysical information because available from the long stretches of active margin that have not yet been targetted for investigation.

Determining if this value is realistic or not can be difficult because rates of melt production under continental arcs are hard to determine. This is because only a small fraction of the melt is actually erupted, while most is intruded into or underplated on to the base of the crust. This is typically hard to resolve seismically and even harder to date. The situation is easier in oceanic arcs, where the whole crustal section is generated by subduction magmatism. If the age of subduction initiation is known then an average rate of production can be calculated. Holbrook *et al.* (1999) estimated long-term magmatic growth rates of 55–82 km^3/my per km of margin for the Aleutians, while Suyehiro *et al.* (1996) indicated long-term average accretion rates of 66 km^3/my per km of margin in the Izu Arc. Both these estimates do not account for the gradual loss of crust by subduction erosion, meaning that the true estimates of magmatic output for these arcs would be higher. However, it should also be recognized that most of the forearc crust in the Tonga, Mariana, Izu, and Bonin arcs is boninitic and produced rapidly after the initiation of subduction, ~45 Ma (Bloomer & Hawkins 1987; Stern & Bloomer 1992). This means that the steady-state average rate of crustal production is likely somewhat below the long-term average derived from seismic measurements. We conclude that the inferred rate of long-term crustal productivity is within error of the best constrained arc magmatic production rates.

Melting in continental active margins necessarily adds new material directly to the continental crustal mass, but the same is not necessarily true for oceanic arcs. Because these are built on oceanic lithosphere this material may be subducted when the arc collides with another trench system along with the lithosphere on which it is built. If oceanic arc crust is not accreted to continental margins during arc-continental collision then the continental mass balance would be disturbed and this subducted arc crust would need to be compensated for by greater production in continental arcs. This seems unlikely to be occurring because continental arc production is typically estimated to be lower than that in oceanic arcs (Plank & Langmuir 1988). For example, Atherton & Petford (1996) estimated production in the Andes be only 8 km^3/m.y./km. Although oceanic arcs account for only 31% of the total active margins in the world our mass budget suggests that 40% (1.2 AU) of global arc melt production occurs along these margins. We estimate global average melt production rates to be 96 and 64 km^3/m.y./km in oceanic and continental arc respectively. If all the production needed to balance global subduction losses (3.0 AU) occurred only in the continental arcs then the average rate of melt production in these settings would increase to an unrealistic 106 km^3/m.y./km. Thus efficient accretion of oceanic arc crust is important to the maintenance of the continental crust, but whether this really occurs or not is open to question. It is noteworthy that there are very few accreted oceanic island arc sections on Earth. Kohistan (Himalayas (Khan *et al.* 1997; Treloar *et al.* 1996)), Alisitos (Baja California (Busby *et al.* 2006)) and Talkeetna (Alaska (DeBari & Coleman 1989)) are noteworthy for being the most complete, while many other examples are small and fragmentary, typically comprising only lavas and volcaniclastic sedimentary rocks. The fate of the oceanic Luzon Arc in the classic arc-continent collision zone of Taiwan is unclear as only a fragment can be seen in the Coastal Ranges. Here we explore its accretion.

Arc Accretion as a Steady-State Process

If arc accretion is to be understood as an integral part of the plate tectonic cycle, and as a key process in maintaining the continental crustal volume then the classic example of Taiwan may be used to quantify the processes that occur when an oceanic arc (Luzon) collides with a passive continental margin (Chemenda *et al.* 1997; Suppe 1981). This type of collision must be relatively common within the life span of the Earth and it has been suggested that it is this process that transforms mafic, depleted arc crust into more siliceous, enriched continental crust (Draut *et al.* 2002). In this scenario high silica, LREE-enriched magmas are injected into the mafic oceanic arc crust as it collides with a passive continental margin. At the same time the mafic/ultramafic lower crust may be subducted along with the mantle lithosphere on which the arc is constructed, made possible by detachment in the weak middle crust.

Arcs may also be accreted to active continental margins and there are examples (e.g., Dras-Kohistan and Talkeetna in southern Alaska) where a complete oceanic crustal section has been transferred to a continental margin when subduction eliminates the oceanic crust between the two arc of the same subduction polarity (Aitchison *et al.* 2000; Clift *et al.* 2005b; DeBari & Coleman 1989; Treloar *et al.* 1996). In both these examples the Moho itself can be observed in the field and there is little doubt that crustal accretion has been efficient. However, the fate of the arc crust during arc-passive margin collision is less clear because such collisions result in the formation of active continental margins following subduction polarity reversal, so that the oceanic plate on which the oceanic arc was constructed is then subducted (Casey & Dewey 1984).

In Taiwan the topographic massif of the North Luzon Arc disappears beneath the SE flank of Taiwan and it is unclear how much arc crust is accreted because the Taiwan ranges themselves expose thick sequences of deformed and metamorphosed Chinese passive margin sedimentary rocks, with only small scattered exposures of volcanic and volcaniclastic rocks found in the eastern Coastal Ranges (Lundberg *et al.* 1997; Song & Lo 2002). In this study we attempt to mass balance the collision in order to assess the efficiency of the accretion process. In doing so we model the collision of Luzon and China as being a steady-state process that is migrating progressively to the SW with time and which started to the NE of the present collision point at some point in the geologic past. We note that some models propose initial Luzon collision to have only initiated around 6–9 Ma, effectively just to the east of the present collision zone, with a transform boundary between the Manila and Ryukyu Trenches prior to collision (Huang *et al.* 2000; Huang *et al.* 2006; Sibuet & Hsu 1997; Suppe 1984). Here we favour a more steady-state collision that may have started much earlier and potentially a long way to the east on modern Taiwan (Clift *et al.* 2003c; Suppe 1984; Teng 1990).

Migration of the arc collision along the margin is then controlled by the speed and obliquity of convergence (Fig. 9). In this scenario along strike variability in the orogen represents different phases in the arc accretion process, with a pre-collisional Luzon arc south of Taiwan, peak collision in the centre of the island and post-collisional orogenic collapse and subduction polarity reversal to the NE of Taiwan. In effect the Luzon arc can be considered to act in a rigid fashion like a snow plough deforming the passive margin of China into an accretionary stack, which then collapsed into the newly formed Ryukyu Trench as the collision point migrated to the SW along the margin (Fig. 10). In this scenario the collapsed orogen comprises slices of Chinese passive margin and the accreted Luzon arc crust, which are then overlain in the Okinawa Trough by sediments eroded from the migrating orogen.

By taking cross sections through the arc in the pre-, syn- and post-collisional stages we can assess to what extent the transfer of arc crust is an efficient process or not.

Fortunately gravity and seismology data allow the large-scale crustal structure of the orogen to be constrained, especially the depth and geometry of the main detachment on which the thrust sheets of passive margin sedimentary rock are carried (Fig. 11)(Carena *et al.* 2002; Chen *et al.* 2004; Lee *et al.* 2002). Similarly, the depth and width of the foreland basin is well characterized by seismic and gravity data (Lin *et al.* 2003). Combined gravity, seismic reflection and refraction surveys constrain the crustal structure in the western Okinawa Trough and Ryukyu Arc, where Moho depths appear to be 25 and 30 km respectively (Kodaira *et al.* 1996; Wang *et al.* 2004). The volume of crust in the colliding arc is less well constrained, but the regional structure across the arc and forearc is known from seismic surveys (Hayes & Lewis 1984), and the crustal thickness of the igneous arc can be estimated at reaching a maximum of ~25 km from gravity data and comparison with seismic data from other oceanic island arcs (Holbrook *et al.* 1999; Suyehiro *et al.* 1996). Sediment volumes on the northern margin of the South China Sea are best characterized from the Pearl River Mouth Basin to the SW of Taiwan where abundant seismic reflection and drilling data provide a good estimate of the total amount of sediment available to be imbricated into the thrust sheets (Clift *et al.* 2004). Our estimates of the crustal volumes are derived from the sections shown in Figure 11 and are listed in Table 4.

By summing the volume of the crustal blocks at each stage of the collision we are able to assess how much material might be subducted during the collision process. This budget is shown graphically in Figure 12. What is most striking is that the great crustal thickness under Taiwan can only be accounted for if the meta-sedimentary thrust sheets that characterize the exposed ranges are underlain by a great thickness of arc crust. The total volume of sediment on the Chinese margin, together with recycled sediments in the accretionary complex west of the Luzon Arc do not come close to explaining the volume of material lying above the basal detachment in the orogen. Although the cross section could be drawn in alternative ways that would change the precise balance between crustal blocks the need to accrete most of the Luzon Arc crust to the Chinese margin to make the sections balance is a common feature of all the reasonable reconstructions. Reducing the volume of accreted arc crust requires that this volume be made up by meta-sedimentary thrust sheets, yet the total volume of sediment on the Chinese margin or in the Manila Accretionary Complex is insufficient to account for this. It is this relative lack of material from which to form the Central Range thrust sheets, together with a relatively voluminous colliding arc that requires the boundary between arc and orogen to dip westwards under the Central Ranges from the Longitudinal Valley. If this boundary is close to vertical then this would require the volume of the thrust sheets to be much greater than all the sediments on the Chinese passive margin and Manila Accretionary Complex from which the range is apparently built. A west-dipping thrust is nonetheless consistent with the structure of the eastern Central Ranges.

In our estimate ~87% of the incoming arc crust is accreted. In addition, some sedimentary material appears to be lost, likely through erosion and recycling back into the pre-collisional accretionary complex, in which only part of the incoming section is imbricated, while some is lost to depth below the arc. The collapse thrust sheets and accreted Luzon arc crust is then required to form the basement to the new Ryukyu Arc. The deformed edge of the Chinese margin is marked by the Taiwan-Sinzi Folded Belt (Fig. 9), located landward of the Okinawa Trough. This means that the Okinawa Trough itself and the arc ridge must be comprised of accreted sediments and arc crust.

Sediment recycling during arc accretion

The degree of sediment recycling during arc accretion can be estimated through a similar mass balancing exercise and through understanding of the rates of rock uplift and exhumation along the strike of Taiwan. Regional trends in rock uplift rates can be determined from the current elevations and the age of the collision, together with estimates for the amount of exhumation derived from the metamorphic grade and fission-track data (Dadson *et al.* 2003; Fuller *et al.* 2006; Liu *et al.* 2000; Tsao *et al.* 1992; Willett *et al.* 2003). Although in some locations modern rates of uplift have been determined by dating terraces (Peng *et al.* 1977; Vita-Finzi & Lin 1998) these are necessarily limited to the coastal regions, mostly in the Coastal Ranges of eastern Taiwan and are not useful for estimating rates of the main accretionary stack. We follow Fuller *et al.* (2006) in placing peak erosion rates at 8 mm/yr., falling to 6 mm/yr. over much of the Central Ranges. These values are consistent with the suspended sediment load calculations of Fuller *et al*. (2003) that predicted rates of 2.2–8.3 mm/yr. Similarly, Dadson *et al*. (2003) used data from river gauging stations to yield an average Central Range erosion rate of ~6 mm/yr.

Exhumation rates driven by erosion reach a peak in the south of the island because rates of rock uplift are highest during the most intense period of collisional compression between Luzon and China; these are partly balanced by erosion driven largely by precipitation, but also by tectonic extension (Crespi *et al.* 1996; Teng *et al.* 2000). Exhumation and vertical uplift rates decrease rapidly toward the northern end of the Central Ranges, and especially around the Ilan Basin (Fig. 13), although active motion along a detachment reversing the Lishan Fault causes increased exhumation in the Hsüehshan Range. Because the rates of exhumation are known from the fission track analysis the total amount of exhumation can be calculated by knowing the duration of the collision, i.e., the speed of arc migration. We show three possible models for sediment accretion and erosion in Figure 14, based on collision starting at 5 Ma, 4 Ma and 3 Ma. The 5 Ma collision age would suggest ~20 km of exhumation, somewhat more than the upper greenschist facies rocks that characterize the Central Ranges (~12–15 km burial), yet this apparent mis-match does not preclude an earlier collision because of the continuous nature in which passive margin sediments may be added to the thrust stack, and recycled at shallower levels, so that while 20 km of erosion occurs this does not result in the progressive unroofing of deeper buried rocks (Willett *et al.* 1993) (Fig. 15).

The 5 Ma collision age is favoured by most recent syntheses (Huang *et al.* 2006), typically based on the ages of cooling, but also on the age of syn-collisional sedimentary rocks exposed in the Coastal Ranges. The Shuilien Conglomerate is dated to start deposition around 3 Ma (Chi *et al.* 1981), yet even this can be considered a minimum age because of the potential for along-strike transport from the location of erosion to the depositional basin.

The most striking result of the sedimentary mass balance is that the volume of meta-sedimentary rocks together with the eroded volumes when compared with the total volumes of possible sediment source seem to require that the rocks now exposed in northern Taiwan, were uplifted and became emergent in a palaeo-southern Taiwan no later than 4 Ma. There is simply insufficient sediment on the northern margin of the South China Sea to account for the orogen and its eroded sediment if uplift and subaerial erosion in the current area of Taiwan started at 5 Ma or before. This means that the speed of collision requires only 4 m.y. for a rock to travel from the southern coast of Taiwan to the collapsing mountains around the Ilan Plain. While some of the eroded sediment is transported into the Okinawa Trough the bulk is recycled back through the foreland basin and south into the Luzon Trench. Because the distal passive margin begins to collide with the Manila Trench south of southern Taiwan we estimate 6–8 m.y. for the duration of the entire accretionary process.

Erosional Control on Crustal Recycling and Thickness

The image we have of the global subduction system is that it both generates new crust principally via arc magmatism and to a lesser extent via subduction accretion, and also returns crustal material to the mantle in tectonically erosive and accretionary active margins. Trench sediment thickness is the primary control on whether a margin is in a state of long-term accretion or tectonic erosion, and this in turn must be controlled by rates of continental erosion. What controls continental erosion is still debated, yet it is clear that tectonically driven rock uplift and climate are key processes (Burbank *et al.* 2003; Dadson *et al.* 2003; Zhang *et al.* 2001). Thus orogeny, uplifting blocks of crust above sea level, increases erosion and feeds sediment to the continental margins where some of it can be recycled into the mantle.

The topography of Earth is dominated by deep oceanic basins that contrast with continents that mostly lie close to sea level, except in regions of recent tectonic deformation (Fig. 16). An analysis of global topography shows that most ocean basins lie 3–7 km below sea level, while the vast majority of continental crust lies <500 m above sea level (Fig. 17). Sedimentary records indicate that the volume of water on the planet's surface has approximately filled the oceanic basins since Precambrian times, neither underfilling nor overspilling by more than ~200 m (Haq *et al.* 1987). This state has lasted likely since the Archaean (Campbell & Taylor 1983; Harrison 1994; McLennan & Taylor 1982; Nisbet 1987). The volume of those basins is determined by the volume, density and thickness of equilibrium continental crust relative to the oceanic crust, but what controls crustal thickness?

Clift & Vannucchi (2004) calculated that at modern rates of plate motion arc magmatism is incapable of producing crust >35 km in tectonically erosive settings (oceanic or continental) because melt production would be incapable of keeping up with mass removal rates. In addition, delamination of dense lower crustal gabbronorite and pyroxenite in active arcs limits the thickness that can formed by magmatism. Behn & Kelemen (2006) demonstrated that such lithologies are convectively unstable relative to the underlying mantle. Seismic velocity data show that most lower crust in modern arcs has seismic velocities (Vp) of more than 7.4 km/s, compared to the Vp >7.4 km/s of the dense gabbronorite. This observation suggests that gravitationally unstable material must founder rapidly on geologic timescales. As a result greater crustal thicknesses would thus require additional tectonically driven horizontal compression.

Although trench processes act as an initial limit on crustal thicknesses the narrow range of 36–41 km found in most continental crust (Christensen & Mooney 1995) must in part reflect the erosion of subaerially exposed crust. Except in regions of long-term extreme aridity (e.g., Atacama Desert)(Hartley *et al.* 2005) orographic rain at mountain fronts will necessarily drive erosion and move crustal material from areas of thickened crust on to continental margins in the form of sediment. Even where climate inhibits erosion the process of continental drift will tend to move crustal blocks out of arid regions and into wetter ones over time periods of 10^7–10^8 yrs, so that eventually tectonically or magmatically thickened crust must be eroded and freeboard reduced to sea level. The "excess" continental crust (i.e., eroded sediment) is returned to the mantle by subduction, either directly to a trench or to a passive margin that is eventually involved in collision with a trench.

No long-term trend in global sea level has been recorded over 10^7–10^9 yrs (Hallam 1992; Haq *et al.* 1987) and there appears to be good evidence for ocean depths in the Archaean being close to modern values (Harrison 1999; Nisbet 1987; Wise 1974). However, there seems no *a priori* reason why the volume of water should not cause sea level to overspill the oceanic basins and flood the continents to a depth of 1 km or more. Conversely, if the volume of water were much less, or the oceanic basins much larger, then sea level would lie well below the level of the continents (Fig. 17). Nonetheless, evidence from the stratigraphic record shows that this has not happened. Harrison (1999) argued that continental freeboard above sea level is controlled by the volume of the water at Earth's surface, which varies over long periods of time (10^7–10^9 yrs). Erosion of elevated topography due to precipitation and glaciation will tend to reduce elevated terrain to sea level (Harrison 1994), thinning the crust as it does so. Conversely, thin, submarine arc crust will tend to be built up to sea level by the compressive tectonic forces favoured by sediment-starved trenches and where coupling between subducting and over-riding plates is stronger (Wells *et al.* 2003), as well as by magmatic accretion. The process is self-limiting because a thickening, uplifting margin will tend to result faster erosion, more sediment in the trench and a reduction in tectonic coupling. Thus continental crustal thickness reflects the combined influence of seawater volume and the ability to subduct significant volumes of crust at both accretionary and erosive margins.

Erosion of Orogenic Topography

The rate at which continental crust is recycled through subduction zones is dependent on how fast orogenic topography can be reduced to sea level. Mountain belts are prone to reactivation after their initial peneplanation, yet they rarely regain major altitude after this initial phase of crustal thinning. The Urals reach heights >1800 m more than 250 m.y. after their formation (Brown *et al.* 2006), yet generally Mesozoic and especially Palaeozoic belts rarely exceed 1 km elevations . The highest mountains on Earth represent Cenozoic and modern plate collisions. Arc-continent collisional orogens reduce to sea level as a result of gravitational collapse into the new trench immediately after the collision point has passed (Clift *et al.* 2003b; Teng 1996), but continent-continent collisions are often different and require extended periods of erosion before equilibrium is attained, i.e. before they are reduced in altitude close to sea level. For example, the mountains formed by the Acadian Orogeny after closure of the Iapetus Ocean reached peak metamorphism around 395 Ma (Armstrong *et al.* 1992) but are truncated by a peneplain erosion unconformity of Late Carboniferous age (~320 Ma) in western Ireland (Graham 1981), suggesting ~75 Ma to remove the excess crust by erosion.

Estimates for the erosion of the Himalaya and Tibet provide an end member example of a very large, long-lived orogen. The volume of eroded rock in the basins around Tibet can be used to determine long-term erosion rates. Eroded rock volumes, with a correction for sediment porosity, are shown in Table 5. These values are determined from regional seismic profiles and are largely from the existing studies of Métivier *et al*. (1999) and Clift *et al*. (2004). As well as the sediments now seen in the major depocentres we estimate those sediments already lost by subduction, especially in the Andaman Arc, where sediment has been subducted at a rate of $1.3\text{x}10^5$ km^3/m.y. in the recent geologic past, although this would have been less earlier since the fan has grown significantly in the Neogene (Métivier *et al*. 1999). We estimate that ~3.2 $\text{x}10^6$ km^3 has been subducted in this way since 50 Ma, assuming no Bengal Fan at that time, and progressive subsequent growth. Subducted losses in the Indus Fan via subduction in the Makran Accretionary Complex would be somewhat less, because that fan has been cut off from the Gulf of Oman since 20 Ma by uplift of Murray Ridge (Mountain & Prell 1990), so that only the Palaeogene erosional record is being lost. The basins of continental Central Asia, including the Tarim, Junngar and Hexi Corridor Basins account for 1.9 x 10^6 km^3 (Métivier *et al.* 1999). The excess crustal mass in Tibet is estimated using a figure of 3.5 x 10^6 km^2 as the area of the plateau, and the figure of 70 km for the crustal thickness, around double the standard equilibrium continental crust.

The average long-term rate of erosion is 0.56 AU since 50 Ma; requiring 220 m.y. to reduce Tibet crust from 70 to 35 km thickness, if the plateau ceased growing today and that long-term rate of erosion was maintained (Fig. 18). Whether this is a reasonable figure is debatable because mass accumulation rates in East Asian marginal seas appear to have increased rapidly after 33 Ma (Clift *et al.* 2004), while recent palaeo-weathering studies from South and East Asia suggest an initial intensification of monsoon summer rains after 22 Ma (Clift & Plumb 2008). As rains are a major trigger for continental erosion much of the sediment now seen around Asia has been eroded since that time. Using 33 and 22 Ma as the start dates for the bulk of the erosion yields average erosion rates of 0.9 and 1.3 AU respectively, and consequently durations of 145 and 97 m.y. to reduce Tibet back to sea level. Thus it appears that little orogenic topography can survive at the Earth's surface beyond ~200 Ma, without the excess crust being recycled to the mantle via subduction zones.

Summary

Geochemical arguments strongly suggest that much of the modern continental crust has been formed in or at least recycled via subduction zones. Subduction zones are also the locations where crustal material is returned to the upper mantle both via tectonic erosion of forearc crust and subduction of sediment in erosive margins, or via the inefficient process of subduction accretion that allows ~83% of the incoming sedimentary column to be subducted over long periods of geologic time (Clift & Vannucchi 2004). Total continental mass subduction rates are approximately 3.0 Armstrong Units (1 AU = 1 km^3/yr), of which 1.65 AU comprises subducted sediments and 1.33 AU tectonically eroded forearc crust (Fig. 18).

Recycling of crust by subduction of passive margins in continent-continent and arc-passive margin collisions is substantially less, averaging 0.4 AU during the Cenozoic.

The process of subduction erosion is still not well understood and may involve both mechanical abrasion of the forearc wedge and/or fluid induced fracturing of the forearc (Vannucchi *et al.* 2008; von Huene *et al.* 2004). What is clear is that erosion can operate in several fashions. Individual margins may retreat landwards in a wholesale, steady-state mode, such as apparently is the case in the South Sandwich, Tonga and Marianas Arcs. Alternatively, trench retreat may occur by erosion of the trenchward forearc coupled with landward underplating, such as seen in the central and northern Andean margin, both associated with trench sediment thicknesses of <1 km. Tectonic erosion is likely a discontinuous process, as suggested by tephra records from offshore Costa Rica (Clift *et al.* 2005a), a region generally associated with long-term tectonic erosion (Vannucchi *et al.* 2001). Geochemical data indicate that subduction erosion in the Central American arc is achieved via periods of slow tectonic erosion interrupted by shorter periods of accelerated erosion, likely driven by seamount subduction, and by periods of sediment accretion.

Subducted crustal losses must be balanced by new production via arc magmatism. Average global melt production rates are 96 and 64 km^3/m.y./km in oceanic and continental arc respectively, close to those estimated by seismic methods, after correction for subduction erosion losses (Holbrook *et al.* 1999; Suyehiro *et al.* 1996). The accretion of oceanic arc crust to continental passive margins during arc-continent collision is crucial to maintaining the volume of the continental crust without excessive melt production in continental arcs. Mass balancing across the Taiwan collision zone suggests that almost 90% of the colliding Luzon Arc crust is accreted to the margin of Asia in that region. The accretion is seen as a steady-state migrating processes, with the collapsed arc and deformed passive margin of China underlying the new Ryukyu forearc ridge and Okinawa Trough. Rates of exhumation and sediment recycling indicate that the subaerial phase of orogenesis spans only ~4 m.y., although initial collision with the deep-water passive margin must have predated that time by 2–3 m.y.

Subduction of sediment in both erosive and inefficient accretionary margins provides a mechanism for returning continental crust to the upper mantle and appears to be fundamental in governing the thickness of the continental crust. Sea level controls rates of continental erosion, reducing topography caused by tectonically over-thickened crust to sea level over timescales of 100–200 Ma. Much of this eroded sediment is delivered directly or indirectly to trenches, allowing its return to the upper mantle. Thus sea level and the volume of water on the Earth's surface controls crustal thicknesses over periods of 10^7–10^9 yrs.

Acknowledgements

PC wishes to thank the Alexander von Humboldt Foundation for support during the writing of this paper at the University of Bremen, as well as the College of Physical Sciences, University of Aberdeen for its generous support. PRIN 2005 Subduction complex dynamics: mass transfer in fossil systems and comparisons with modern examples, funded PV. We thank Dennis Brown and David Tappin for their constructive comments in review for improving the manuscript.

Figure Captions

Figure 1. Schematic map of the global subduction system showing the distribution of accreting versus eroding subduction zones. Accretionary margins are shown with filled barbs on the plate boundary, while empty barbs mark erosive margins. Modified after Clift & Vannucchi (2004), reproduced with permission of the American Geophysical Union.

Figure 2. Schematic cartoons showing the features common to the two basic types of active margin from Clift & Vannucchi (2004). (A) Accretionary margins, such as Cascadia, are characterized by forearc regions comprised thrusted and penetratively deformed trench and oceanic sediments that often develop mud diapirism and volcanism due to sediment over-pressuring. Gas hydrate zones are also commonly associated with structures in the wedge, (B) in contrast erosive plate margins, such as Tonga, are marked by steep trench slopes, comprised of volcanic, plutonic and mantle rocks. Sedimentary rocks are typically limited to the forearc basin, where they may be faulted but are not strongly sheared in the fashion of an accretionary wedge. In the Marianas serpentinite mud volcanism is recorded. Reprinted with permission from the American Geophysical Union.

Figure 3. Diagrams showing the relationship of (A) orthogonal convergence rates and (B) trench sediment thicknesses to the net crustal growth or loss along the global active margins, from Clift & Vannucchi (2004). Modified with permission from American Geophysical Union. Large circles show erosive plate margins for which a trench retreat is well defined, compared to the small circles representing margins for which tectonic erosion rates are inferred. ALE = Aleutians; AND = Andaman; BC = British Columbia; COS = Costa Rica;

ECU = Ecuador; GUA = Guatemala; JAV = Java; KER = Kermadec; KUR = Kurile; LA = Lesser Antilles; LUZ = Luzon-Philippine; MAK = Makran; MED = Mediterranean; MEX = Mexico; MIN = Mindanao; NAN = Nankai; NC = Northern Chile; NIC = Nicaragua; PER = Peru; RYU = Ryukyu; SC = Southern Chile; SOL = Solomons; SS = South Sandwich; SUM = Sumatra; TAI = Taiwan; TON = Tonga; WAS = Washington-Oregon.

Figure 4. (A) Multichannel seismic reflection profile HIG-14, with (B) close-up of Lima Basin, and (C) after depth conversion and interpretation of age structure, largely correlated from ODP Site 679 located at the landward end of the profile.

Figure 5. Bathymetric map of the eastern Pacific offshore Peru and Chile showing the locations of the basins discussed in the text, as well as the major bathymetric ridges now in collision with the Andean margin. Depth data are from GEBCO. Depth contours in 500 m intervals. Boxes show regions of detailed offshore geophysical (seismic and bathymetric mapping) surveys. Re-printed with permission from Geological Society of America (Clift & Hartley 2007).

Figure 6. Reconstructed depth to basement for a series of Andean forearc sedimentary basins during the Cenozoic showing the general slow rate of subsidence consistent with long-term net mass loss during subduction erosion. Lima Basin (ODP Site 679 on the inner shelf, and ODP Site 682 on the trench slope) reconstruction is from Clift *et al.* (2003). Pisco Basin data are taken from Dunbar *et al.* (1990) and Tsuchi (1992). Mejillones Peninsula data are from Hartley & Jolley (1995), Krebs *et al.* (1992), Ortlieb *et al.* (1996) and Ibaraki (2001). Caldera and Carrizalillo reconstructed are from Marquardt *et al.* (2004) and Le Roux *et al.* (2005)

(2005) respectively. Height of black vertical bars shows the magnitude of the uncertainties in palaeo-water depth. Altered from Clift & Hartley (2007) and with permission from Geological Society of America.

Figure 7. Cartoon showing the alternative modes of subduction erosion. (A) shows the slower and non-steady state style of erosion as typified by Neogene northern and central Andes in which erosion is concentrated close to the trench, while the coast remains approximately stationary. Trench retreat is accommodated by steepening of the forearc taper (B) shows the fast, steady-state mode of erosion, apparently operating in the western Pacific, where taper angle remains constant and trench retreat rate corresponds to loss of complete crustal thickness.

Figure 8. (A) Plot of ε_{Nd} and δ^7Li shows that while the majority of tephra glasses at ODP Sites 1039, 1041 and 1043 could be explain by a petrogenesis mixing recycled MORB crust and subducted sediments, an additional, likely forearc component is required. Sediment data from Chan and Kastner (2000) and Kelly (2003). (B) Diagrams showing the evolving Li and Nd isotopic composition of Costa Rican tephras since 2.5 Ma. Histogram of ε_{Nd} values for modern Costa Rica is from GEOROC. Modern δ^7Li value for Arenal volcano from Chan *et al.* (1999) , Nd data from Feigenson *et al.* (2004). Sediment proportion of petrogenesis is calculated from end member mixing model based on Nd isotopes. Diagram shows the strong temporal variability in the degree of sediment and forearc crustal recycling, likely linked to seamount collision.

Figure 9. Bathymetric map of the Taiwan region showing the collisional orogen, the opposing subduction polarities and the Okinawa Trough opening in the wake of orogenic collapse. The numbered lines adjacent to the plate boundary show the inferred time of peak arc collision between the Luzon Arc and the passive margin of China in the past and future. Map is labelled to show the different stage of arc-continent collision along strike. Dashed line shows location of the Taiwan-Sinzi Foldbelt, interpreted as remnants of the former collisional orogen, while the grey line shows the location of the modern arc volcanic front, focused by extension in the Okinawa Trough close to Taiwan (re-printed from Clift *et al.* 2003).

Figure 10. Cartoon showing the proposed tectonic model for Luzon Arc collision in Taiwan. Arc crust (cross pattern) acts much like a snow plough, deforming and uplifting sediments of the Chinese passive margin (dotted pattern). As the collision point migrates along the margin the compressive stress is released and the orogen collapses to form a basin, subsequently infilled by sediment, largely eroded from the orogen (horizontal shading).

Figure 11. Cross sections through the Taiwan collision zone, south of the collision zone, at the collisional maximum in central Taiwan and across the Okinawa Trough and Ryukyu forearc, interpreted to be in a post-collisional state. Crustal structure under Taiwan is inferred from the seismic evidence of Carena *et al.* (2002) shown as black and grey dots projected on to the section from a number of major faults in the central Taiwan region. See Figure 9 for locations of the sections.

Figure 12. Diagram showing the relative volumes of accreted and subducted arc crust, versus eroded sediment in the Taiwan collision zone. The figure shows the relatively high efficiency

of the accretion process in transferring oceanic arc crust to the Asian margin (88%). Crustal volumes are derived from the balanced cross sections shown in Figure 11.

Figure 13. (A) Simplified geological map of Taiwan showing the map tectonic units that comprise the island and the location of the Ilan Basin along the strike of the Lishan Fault, which separates the Hsüehshan and Backbone Ranges. (B) Diagram showing the rates of erosion along the Central Ranges of Taiwan, running south to north. Rates are based on fission track analysis of Willett *et al.*(2003). Modelled depths of erosion infer a start of collision at 5, 3 and 2 Ma at the northern end of Taiwan and a propagating collisional orogen younging to the south.

Figure 14. Diagram showing the balance between the sediments and sedimentary rocks available to form the Taiwan Orogen within the Luzon forearc and Chinese passive margin and the measured volume of the Taiwan thrust sheets and eroded volumes predicted for collision starting at different times for that point on the Luzon Arc now directly under the northern tip of Taiwan. The generally accepted 5 Ma collision age appears to require more material than is actually available in the system.

Figure 15. Diagram redrawn from Willett *et al.* (1993) showing that crust from the subducting plate (China) is fluxed through the orogen, so that erosion at the mountain front can continue indefinitely without exposing any deeper level material at any given point. This type of horizontal transport must be occurring if the 20 km of erosion has occurred in the Central Ranges without higher grade metamorphic rocks being exposed.

Figure 16. Hypsometry of the Earth, showing the bipolar distribution between ocean basins and continental crust that shows a particular sharp maximum close to sea level, representing the equilibrium state of the continental crust and equivalent to a thick of ~36 km with normal density structure (Rudnick & Fountain 1995).

Figure 17. Cartoon showing the two states of continental crust at subduction margins. Thin crust lying below sea-level is not eroded and is built up by voluminous melt production, while subaerial continental arcs have low melt production and are continuously eroded to sea-level, even when active.

Figure 18. Diagram showing the comparative rates of sediment recycling in subduction zones relative to tectonic erosion, arc magmatism, ocean island basalt (OIB) magmatism, subduction accretion and the erosional flux from Asia.

Table 1. Summary of the lengths of Cenozoic mountain belts along which passive margins have been subducted since 65 Ma, together with an estimate of the subducted crustal volumes assuming 50% of the margins are volcanic and 50% non-volcanic.

Table 2. Summary of some of the major tectonic characteristics of the world's subduction zones, shown in Figure 1. Values are modified after those presented by Clift & Vannucchi (2004), especially with regard to the North Chile and Peruvian margins. Magmatic production rates are set to balance subducted losses and are scaled to reflect convergence velocity.

Table 3. Rates of mass recycling for major crustal mass repositories. AU = Armstrong Unit ($1\ km^3$/yr.). Arc magmatic production rate is calculated to match the degree of crustal subduction (sediment and forearc crust). Subduction accretion rate is from Clift & Vannucchi (2004). Mid Ocean Ridge Basalt (MORB) production rate is from Dick *et al.* (2003). Ocean Island Basalt (OIB) production is from S. Hart (pers. comm., 2006). Total river discharge is from Milliman (1997). Asian Cenozoic erosion rate is from Clift *et al.* (2004).

Table 4. Estimates of the volumes of crustal material found in the colliding Luzon Arc, the Taiwan Orogen and in the post-collisional Ryukyu-Okinawa Arc system, together with total erosion estimates for the Taiwan Orogen estimated assuming different ages for the start of collision at 5, 3 and 2 Ma.

Table 5. Volumes of basins in Asia that have largely been filled by erosion of the Himalaya and Tibetan Plateau (data compiled from Clift *et al.* (2004) for the marine and foreland basin and from Métivier *et al.* (1999) for the basins of Central Asia). This volume of sediment can be used to calculate long-term average rates of sediment production. Given the modern size of Tibet and the known "excess" crustal thickness above average continental values the time needed to remove Tibet can be estimated. Erosion has been much faster since ~33 Ma and thus a range of possible values can be calculated assume erosion starting after collision ~50 Ma or just since 33 Ma.

Table 6. Estimates average rates of erosion for the Himalaya and Tibetan Plateau assuming uplift and erosion started at 50 Ma, close to time of collision, and alternatively at 33 Ma when erosion rates are seen to greatly accelerate in Asia (Clift *et al.* 2004).

References

Aitchison, J. C., Badengzhu, D., Davis, A. M., Liu, J., Luo, H., Malpas, J., McDermid, I. M. C., Wu, H., Ziabrev, S. & Zhou, M. F. 2000. Remnants of a Cretaceous intra-oceanic subduction system within the Yarlung–Zangbo suture (southern Tibet). *Earth and Planetary Science Letters,* **183**, 231– 244.

Albarede, F. & Brouxel, M. 1987. The Sm/Nd secular variation of the continental crust and the depleted mantle. *Earth and Planetary Science Letters,* **82**, 25-35.

Armstrong, R. L. & Harmon, R. S. 1981. Radiogenic Isotopes: The case for crustal recycling on a near-steady-state no-continental-growth Earth. *Philosophical Transactions of the Royal Society of London. Series A, Mathematical and Physical Sciences,* **301**(1461), 443-472.

Armstrong, T. R., Tracy, R. J. & Hames, W. E. 1992. Contrasting styles of Taconian, Eastern Acadian and Western Acadian metamorphism, central and western New England. *Journal of Metamorphic Geology,* **10**, 415–426.

Atherton, M. P. & Petford, N. 1996. Plutonism and the growth of Andean crust at 9 degrees S from 100 to 3 Ma. *Journal of South American Earth Sciences,* **9**, 1–9.

Bangs, N. L. B., Gulick, S. P. S. & Shipley, T. H. 2006. Seamount subduction erosion in the Nankai Trough and its potential impact on the seismogenic zone. *Geology,* **34**, 701–704, doi: 10.1130/G22451.1.

Barth, M. G., McDonough, W. F. & Rudnick, R. L. 2000. Tracking the budget of Nb and Ta in the continental crust. *Chemical Geology,* **165**, 197–213.

Behn, M. & Kelemen, P. 2006. Stability of arc lower crust; insights from the Talkeetna Arc section, south central Alaska, and the seismic structure of modern arcs. *Journal of Geophysical Research,* **111**(B11), doi:10.1029/2006JB004327.

Bloomer, S. H. & Hawkins, J. W. 1987. Petrology and geochemistry of boninite series volcanic rocks from the Mariana trench. *Contributions to Mineralogy and Petrology,* **97**, 361–377.

Boher, M., Abouchami, W., Michard, A., Albarede, F. & Arndt, N. T. 1992. Crustal growth in West Africa at 2.1 Ga. *Journal of Geophysical Research,* **97**, 345–36.

Bowring, S. A. & Housh, T. 1995. The Earth's early evolution. *Science,* **269**, 1535–1540.

Brown, D., Puchkov, V., Alvarez-Marron, J., Bea, F. & Perez-Estaun, A. 2006. Tectonic processes in the Southern and Middle Urals; an overview. In *European lithosphere dynamics.* (Eds, D. G. Gee and R. A. Stephenson), London: Geological Society, Memoirs, 32, pp. 407-419.

Burbank, D. W., Blythe, A. E., Putkonen, J., Pratt-Sitaula, B., Gabet, E., Oskins, M., Barros, A. & Ojha, T. P. 2003. Decoupling of erosion and precipitation in the Himalayas. *Nature,* **426**, 652–655.

Busby, C., Fackler Adams, B., Mattinson, J. & Deoreo, S. 2006. View of an intact oceanic arc, from surficial to mesozonal levels: Cretaceous Alisitos arc, Baja California. *Journal of Volcanology and Geothermal Research,* **149**, 1– 46.

Campbell, I. H. & Taylor, S. R. 1983. No water, no granites; no oceans, no continents. *Geophysical Research Letters,* **10**(11), 1061–1064.

Carena, S., Suppe, J. & Kao, H. 2002. Active detachment of Taiwan illuminated by small earthquakes and its control of first-order topography. *Geology,* **30**, 935–938.

Carr, M. J., Feigenson, M. D., Patino, L. C. & Walker, J. A. 2003. Volcanism and geochemistry in Central America: Progress and problems, in Inside the Subduction Factory. (Ed, J. Eiler), Washington, D.C: American Geophysical Union, Geophysical Monograph, 138, pp. 153–174.

Casey, J. F. & Dewey, J. F. 1984. Initiation of subduction zones along transform and accreting plate boundaries, triple-junction evolution, and forearc spreading centres-implications for ophiolitic geology and obduction. In *Ophiolites and Oceanic Lithosphere.* (Eds, I. G. Gass, S. J. Lippard and A. W. Shelton), London: Geological Society, Special Publication, 13, pp. 269–290.

Chan, L.-H., Leeman, W. P. & You, C. F. 1999. Lithium isotopic composition of Central American Volcanic Arc lavas: Implications for modification of subarc mantle by slab-derived fluids. *Chemical Geology,* **160**, 255–280.

Chan, L.-H. & Kastner, M. 2000. Lithium isotopic compositions of pore fluids and sediments in the Costa Rica subduction zone; implications for fluid processes and sediment contribution to the arc volcanoes. *Earth and Planetary Science Letters,* **183**, 275–290.

CHEMENDA, A. I., YANG, R. K., HSIEH, C. H. & GROHOLSKY, A. L. 1997. Evolutionary model for the Taiwan collision based on physical modeling. *Tectonophysics,* **274**, 253–274.

CHEN, P.-F., HUANG, B.-S. & LIANG, W.-T. 2004. Evidence of a slab of subducted lithosphere beneath central Taiwan from seismic waveforms and travel times. *Earth and Planetary Science Letters,* **229**, 61–71.

CHI, W. R., NAMSON, J. & SUPPE, J. 1981. Stratigraphic record of plate interactions in the Coastal Range of eastern Taiwan. *Geological Society of China Memoir,* **4**, 155–194.

CHRISTENSEN, N. I. & MOONEY, W. D. 1995. Seismic velocity structure and composition of the continental crust; a global view. *Journal of Geophysical Research,* **100**, 9761–9788.

CLIFT, P. & VANNUCCHI, P. 2004. Controls on tectonic accretion versus erosion in subduction zones; implications for the origin and recycling of the continental crust. *Reviews of Geophysics,* **42**, no.2, 31.

CLIFT, P. D. & MACLEOD, C. J. 1999. Slow rates of subduction erosion estimated from subsidence and tilting of the Tonga forearc. *Geology,* **27**(5), 411-414.

CLIFT, P. D., PECHER, I., KUKOWSKI, N. & HAMPEL, A. 2003a. Tectonic erosion of the Peruvian forearc, Lima Basin, by subduction and Nazca Ridge collision. *Tectonics,* **22, 1023**, doi:10.1029/2002TC001386.

CLIFT, P. D., SCHOUTEN, H. & DRAUT, A. E. 2003b. A general model of arc-continent collision and subduction polarity reversal from Taiwan and the Irish Caledonides. In *Intra-Oceanic Subduction Systems; Tectonic and Magmatic Processes.* (Eds, R. D. LARTER and P. T. LEAT), London: Geological Society, Special Publication, 219, pp. 81-98.

CLIFT, P. D., SCHOUTEN, H. & DRAUT, A. E. 2003c. A general model of arc-continent collision and subduction polarity reversal from Taiwan and the Irish Caledonides. In *Intra-Oceanic Subduction Systems; Tectonic and Magmatic Processes.* (Eds, R. D. LARTER and P. T. LEAT), London: Geological Society, special publication, 219, pp. 81–98.

CLIFT, P. D., LAYNE, G. D. & BLUSZTAJN, J. 2004. Marine sedimentary evidence for monsoon strengthening, Tibetan uplift and drainage evolution in east Asia. In *Continent-Ocean Interactions in the East Asian Marginal Seas.* (Eds, P. CLIFT, W. KUHNT, P. WANG and D. HAYES), Washington, DC: American Geophysical Union, Geophysical Monograph, 149, pp. 255-282.

CLIFT, P. D., CHAN, L.-H., BLUSZTAJN, J., LAYNE, G. D., KASTNER, M. & KELLY, R. K. 2005a. Pulsed subduction accretion and tectonic erosion reconstructed since 2.5 Ma from the tephra record offshore Costa Rica. *Geochemistry, Geophysics, Geosystems,* **6**(Q09016), doi:10.1029/2005GC000963.

CLIFT, P. D., PAVLIS, T., DEBARI, S. M., DRAUT, A. E., RIOUX, M. & KELEMEN, P. B. 2005b. Subduction erosion of the Jurassic Talkeetna-Bonanza Arc and the Mesozoic accretionary tectonics of western North America. *Geology,* **33**(11), 881-884.

CLIFT, P. D. & HARTLEY, A. 2007. Slow rates of subduction erosion along the Andean margin and reduced global crustal recycling. *Geology,* **35**, 503–506.

CLIFT, P. D. & PLUMB, R. A. 2008. *The Asian Monsoon: Causes, History and Effects*. Cambridge: Cambridge University Press, in press.

CRESPI, J., CHAN, Y. C. & SWAIM, M. 1996. Synorogenic extension and exhumation of the Taiwan hinterland. *Geology,* **24**, 247–250.

DADSON, S., HOVIUS, N., CHEN, H., DADE, W. B., HSIEH, M. L., WILLETT, S., HU, J. C., HORNG, M. J., CHEN, M. C., STARK, C. P., LAGUE, D. & LIN, J. C. 2003. Links between erosion, runoff variability and seismicity in the Taiwan orogen. *Nature,* **426**, 648–651.

DEBARI, S. M. & COLEMAN, R. G. 1989. Examination of the deep levels of an island arc: evidence from the Tonsina Ultramafic-Mafic assemblage, Tonsina, Alaska. *Journal of Geophysical Research,* **94**, 4373–4391.

DEWEY, J. F. & WINDLEY, B. F. 1981. Growth and differentiation of the continental crust. *Philosophical Transactions of the Royal Society, London A,* **301**, 189–206.

DICK, H. J. B., LIN, J. & SCHOUTEN, H. 2003. An ultraslow-spreading class of ocean ridge. *Nature,* **426**, 405-412.

DRAUT, A. E., CLIFT, P. D., HANNIGAN, R. E., LAYNE, G. & SHIMIZU, N. 2002. A model for continental crust genesis by arc accretion; rare earth element evidence from the Irish Caledonides. *Earth and Planetary Science Letters,* **203**(3-4), 861-877.

DUNBAR, R. B., MARTY, R. C. & BAKER, P. A. 1990. Cenozoic marine sedimentation in the Sechura and Pisco basins, Peru. *Palaeogeography Palaeoclimatology Palaeoecology,* **77**, 235–261.

ELLAM, R. M. & HAWKESWORTH, C. J. 1988. Is average continental crust generated at subduction zones? *Geology,* **16**, 314–317.

Elliott, T., Zindler, A. & Bourdon, B. 1999. Exploring the kappa conundrum; the role of recycling in the lead isotope evolution of the mantle. *Earth and Planetary Science Letters,* **169**, 129–145.

Feigenson, M. D., Carr, M. J., Maharaj, S. V., Juliano, S. & Bolge, L. L. 2004. Lead isotope composition of Central American volcanoes: Influence of the Galapagos plume. *Geochemistry Geophysics Geosystems,* **5**(Q06001), doi:10.1029/ 2003GC000621. .

Fuller, C. W., Willett, S. D., Hovius, N. & Slingerland, R. 2003. Erosion rates for Taiwan mountain basins: new determinations from suspended sediment records and a stochasticmodel of their variation. *Journal of Geology,* **111**, 71–87.

Fuller, C. W., Willett, S. D., Fisher, D. & Lu, C. Y. 2006. A thermomechanical wedge model of Taiwan constrained by fission-track thermochronometry. *Tectonophysics,* **425**(1-4), 1-24.

Gao, S., Rudnick, R. L. & Yuan, H.-L. 2004. Recycling lower continental crust in the North China craton. *Nature,* **432**, 892–897.

Goldstein, S. L., Arndt, N. T. & Stallard, R. F. 1997. The history of a continent from U-Pb ages of zircons from Orinoco River sand and Sm-Nd isotopes in Orinoco Basin river sediments. *Chemical Geology,* **139**, 271–286.

Graham, J. R. 1981. Fluvial sedimentation in the Lower Carboniferous of Clew Bay, County Mayo, Ireland. *Sedimentary Geology,* **30**(3), 195-211.

Hallam, A. 1992. *Phanerozoic sea-level changes*. New York, NY: Columbia University Press, p. 266,

Hampel, A. 2002. The migration history of the Nazca Ridge along the Peruvian active margin: a re-evaluation. *Earth and Planetary Science Letters,* **203**(2), 665-679.

Haq, B. U., Hardenbol, J. & Vail, P. R. 1987. Chronology of fluctuating sea levels since the Triassic. *Science,* **235**, 1156–1167.

Harrison, C. G. A. 1994. Rates of continental erosion and mountain building. *Geologische Rundschau,* **83**, 431–437.

Harrison, C. G. A. 1999. Constraints on ocean volume change since the Archean. *Geophysical Research Letters,* **26**, 1913–1916.

Hartley, A. J. & Jolley, E. J. 1995. Tectonic implications of Late Cenozoic sedimentation from the Coastal Cordillera of northern Chile (22–24˚S). *Journal of the Geological Society,* **152**, 51– 63.

Hartley, A. J., Chong, G., Houston, J. & Mather, A. E. 2005. 150 million years of climatic stability; evidence from the Atacama Desert, northern Chile. *Journal of the Geological Society,* **162**, 421–424.

Hawkesworth, C. J. & Kemp, A. I. S. 2006. Evolution of the continental crust. *Nature,* **443**, 811–817, doi:10.1038/nature05191.

Hayes, D. E. & Lewis, S. D. 1984. A geophysical study of the Manila Trench, Luzon, Philippines; 1, Crustal structure, gravity, and regional tectonic evolution. *Journal of Geophysical Research,* **89**, 9171–9195.

Hilde, T. W. C. 1983. Sediment subduction versus accretion around the Pacific. *Tectonophysics,* **99**, 381–397.

Hildebrand, R. S. & Bowring, S. A. 1999. Crustal recycling by slab failure. *Geology,* **27**, 11–14.

Holbrook, W. S., Lizarralde, D., McGeary, S., N., B. & J., D. 1999. Structure and composition of the Aleutian island arc and implications for continental crustal growth. *Geology,* **27**, 31–34.

Huang, C. Y., Yuan, P. B., Lin, C. W. & Wang, T. K. 2000. Geodynamic processes of Taiwan arc-continent collision and comparison with analogs in Timor, Papua New Guinea, Urals and Corsica. *Tectonophysics, ,* **325**, 1–21, doi: 10.1016/S0040-1951(00)00128-1.

Huang, C. Y., Yuan, P. B. & Tsao, S. H. 2006. Temporal and spatial records of active arc-continent collision in Taiwan: A synthesis. *Geological Society of America Bulletin,* **118**, 274–288.

Ibaraki, M. 2001. Neogene planktonic foraminifera of the Caleta Herradura de Mejillones section in northern Chile: Biostratigraphy and paleoceanogoraphic implications. *Micropalaeontology,* **47**, 257–267.

Jacobsen, S. B. 1988. Isotopic constraints on crustal growth and recycling. *Earth and Planetary Science Letters,* **90**, 315–329.

Johnson, M. R. W. 2002. Shortening budgets and the role of continental subduction during the India-Asia collision. *Earth-Science Reviews,* **59**, 101–123.

Kelly, R. K. 2003. Subduction Dynamics at the Middle America Trench: New constraints from swath bathymetry, multichannel seismic data, and 10Be, Ph.D. thesis, Massachusetts Institute of Technology/Woods Hole Oceanographic Institution, pp. 334.

KHAN, M. A., STERN, R. J., GRIBBLE, R. F. & WINDLEY, B. F. 1997. Geochemical and isotopic constraints on subduction polarity, magma sources, and palaeogeography of the Kohistan intra-oceanic arc, northern Pakistan Himalaya. *Journal of the Geological Society,* **154**, 935-946.

KIMURA, G., SILVER, E. A., BLUM, P. & ODP LEG 170 SCIENTIFIC PARTY 1997. Proceedings of the Ocean Drilling Program, Initial Report, 170, College Station, Texas: Ocean Drilling Program.

KODAIRA, S., IWASAKI, T., URABE, T., KANAZAWA, T., EGLOFF, F., MAKRIS, J. & SHIMAMURA, H. 1996. Crustal structure across the middle Ryukyu Trench obtained from ocean bottom seismographic data. *Tectonophysics,* **263**, 39–60.

KREBS, W. N., ALEMAN, A. M., PADILLA, H., ROSENFELD, J. H. & NIEMEYER, H. 1992. Age and paleoceanographic significance of the Caleta Herradura diatomite, Peninsula de Mejillones, Antofagasta, Chile. *Revista Geologica de Chile,* **19**, 75–81.

LAMB, S. & DAVIS, P. 2003. Cenozoic climate change as a possible cause for the rise of the Andes. *Nature,* **425**, 792–797.

LAURSEN, J., SCHOLL, D. W. & VON HUENE, R. 2002. Neotectonic deformation of the central Chile margin: Deepwater forearc basin formation in response to hot spot ridge and seamount subduction. *Tectonics,* **21, 1038**(5), doi:10.1029/2001TC901023.

LE PICHON, X., HENRY, P. & LALLEMANT, S. 1993. Accretion and erosion in subduction zones: The role of fluids. *Annual Reviews of Earth and Planetary Sciences,* **21,** , 307–331.

LE ROUX, J. P., GÓMEZA, C. V., FENNER, C. J., MIDDLETON, H., MARCHANT, M., BUCHBINDER, B., FRASSINETTI, D., MARQUARDT, C., GREGORY-WODZICKI, K. M. & LAVENU, A. 2005. Neogene-Quaternary coastal and offshore sedimentation in north central Chile: Record of sea-level changes and implications for Andean tectonism. *Journal of South American Earth Sciences,* **19**, 83–98.

LEE, J. C., CHU, H.-T., ANGELIER, J., CHAN, Y.-C., HU, J.-C., LU, C.-Y. & RAU, R.-J. 2002. Geometry and structure of northern surface ruptures of the 1999 Mw = 7.6 Chi-Chi, Taiwan earthquake: influence from inherited fold belt structures. . *Journal of Structural Geology,* **24**, 173–192.

LEECH, M. & STOCKLI, D. F. 2000. The late exhumation history of the ultrahigh-pressure Maksyutov Complex, south Ural Mountains, from new apatite fission track data. *Tectonics,* **19**(1), 153-167.

Leeman, W. P., Carr, M. J. & Morris, J. D. 1994. Boron geochemistry of the Central American volcanic arc; constraints on the genesis of subduction-related magmas. *Geochimica et Cosmochimica Acta,* **58**, 149–168.

Lin, A. T., Watts, A. B. & Hesselbo, S. P. 2003. Cenozoic stratigraphy and subsidence history of the South China Sea margin in the Taiwan region. *Basin Research,* **15**, 453–478.

Liu, T. K., Chen, Y. G., Chen, W. S. & Jiang, S. H. 2000. Rates of cooling and denudation of the Early Penglai Orogeny, Taiwan, as assessed by fission-track constraints. *Tectonophysics,* **320**, 69–82.

Lundberg, N., Reed, D. L., Liu, C.-S. & Lieske, J. 1997. Forearc-basin closure and arc accretion in the submarine suture zone south of Taiwan. *Tectonophysics,* **274**, 5–23.

Marquardt, C., Lavenu, A., Ortlieb, L., Godoya, E. & Comte, D. 2004. Coastal neotectonics in southern Central Andes; uplift and deformation of marine terraces in northern Chile (27°S). *Tectonophysics,* **394**, 193–219.

McLennan, S. M. & Taylor, S. R. 1982. Geochemical constraints on the growth of the continental crust. *Journal of Geology,* **90**, 347–361.

Melnick, D. & Echtler, H. P. 2006. Inversion of forearc basins in south-central Chile caused by rapid glacial age trench fill. *Geology,* **34**, 709–712.

Meschede, M., Zweigel, P. & Kiefer, E. 1999. Subsidence and extension at a convergent plate margin: Evidence for subduction erosion off Costa Rica,. *Terra Nova,* **11**, 112– 117.

Metivier, F., Gaudemer, Y., Tapponnier, P. & Klein, M. 1999. Mass accumulation rates in Asia during the Cenozoic. *Geophysical Journal International,* **137**(2), 280-318.

Miller, H. 1970. *Vergleichende Studien an praemesozoischen Gesteinen Chiles unter besonderer Beruecksichtigung ihrer Kleintektonik.* Stuttgart: Schweizerbart'sche Verlagsbuchhandlung, p. 36,

Milliman, J. D. 1997. Fluvial sediment discharge to the sea and the importance of regional tectonics. In *Tectonic Uplift and Climate Change.* (Ed, W. F. Ruddiman), New York: Plenum Press, pp. 239-257.

Moorbath, S. 1978. Age and isotope evidence for the evolution of the continental crust. *Philosophical Transactions of the Royal Society, London, A,* **288**, 401–413.

Morris, J., Valentine, R. & Harrison, T. 2002. 10Be imaging of sediment accretion and subduction along the northeast Japan and Costa Rica convergent margins. *Geology,* **30**, 59–62.

Mountain, G. S. & Prell, W. L. 1990. A multiphase plate tectonic history of the southeast continental margin of Oman. In *The Geology and Tectonics of Oman.* (Eds, A. H. F. Robertson, M. P. Searle and A. C. Ries), London: Geological Society, Special Publication, 49, pp. 725–743.

Murauchi, S. 1971. The renewal of island arcs and the tectonics of marginal seas. In *Island arc and marginal seas.* (Eds, S. Asano and G. B. Udintsev), Japan: Tokai University Press, pp. 39–56.

Nisbet, E. G. 1987. *The young Earth; an introduction to Archaean geology*. London: Allen & Unwin, p. 402,

O'Nions, R. K., Evensen, N. M. & Hamilton, P. J. 1979. Geochemical modelling of mantle differentiation and crustal growth. *Journal of Geophysical Research,* **84**, 6091–6101.

Ortlieb, L., Zazo, C., Goy, J. L., Dabrio, C. & Macharé, J. 1996. Pampa del Palo; an anomalous composite marine terrace on the uprising coast of southern Peru. *Journal of South American Earth Sciences,* **9**, 367–379.

Patino, L. C., Carr, M. J. & Feigenson, M. D. 2000. Local and regional variations in Central American arc lavas controlled by variations in subducted sediment input. *Contributions to Mineralogy and Petrology,* **138**, 265–283.

Peng, T.-H., Li, Y.-H. & Wu, F. T. 1977. Tectonic uplift rates of the Taiwan Island since the early Holocene. *Geological Society of China Memoir,* **2**, 57–69.

Plank, T. & Langmuir, C. H. 1988. An evaluation of the global variations in the major element chemistry of arc basalts. *Earth and Planetary Science Letters,* **90**, 349–370.

Platt, J. P. 1986. The mechanics of frontal imbrication: A first-order analysis. *Geologische Rundschau,* **77**, 577–589.

Ranero, C. R. & von Huene, R. 2000. Subduction erosion along the Middle America convergent margin. *Nature,* **404**(6779), 748-752.

Ratschbacher, L., Hacker, B. R., Webb, L. E., McWilliams, M., Ireland, T., Dong, S., Calvert, A., Chateigner, D. & Wenk, H.-R. 2000. Exhumation of the ultrahigh-pressure continental crust in east central China; Cretaceous and Cenozoic unroofing and the Tan-Lu Fault. *Journal of Geophysical Research,* **105**(B6), 13,303-13,338.

Reagan, M., Morris, J., Herrstrom, E. & Murrell, M. 1994. Uranium series and beryllium isotopic evidence for an extended history of subduction modification of the mantle below Nicaragua. *Geochimica et Cosmochimica Acta,* **58**, 4199–4212.

Rudnick, R. L. 1995. Making continental crust. *Nature,* **378**, 573–578.

Rudnick, R. L. & Fountain, D. M. 1995. Nature and composition of the continental crust; a lower crustal perspective. *Reviews of Geophysics,* **33**(267–309).

Rutland, R. W. R. 1971. Andean orogeny and ocean floor spreading. *Nature,* **233**, 252-255.

Ryan, H. F. & Scholl, D. W. 1993. Geologic implications of great interplate earthquakes along the Aleutian arc. *Journal of Geophysical Research,* **98**(B12), 22,135–22,146.

Scheuber, E. & Reutter, K. J. 1992. Magmatic arc tectonics in the Central Andes between 21° and 25°S. *Tectonophysics,* **205**, 127–140, doi: 10.1016/0040-1951(92)90422-3.

Scholl, D. W., Marlow, M. S. & Cooper, A. K. 1977. Sediment subduction and offscraping at Pacific margins. In: (eds.) Island arcs, deep sea trenches and back-arc basins. (Eds, M. Talwani and W. C. Pitman): American Geophysical Union, Maurice Ewing Series, 1, pp. 199–210.

Schubert, G. & Reymer, A. P. S. 1985. Continental volume and freeboard through geological time. *Nature,* **316**, 336–339.

Shipley, T. H., McIntosh, K. D., Silver, E. A. & Stoffa, P. L. 1992. Three-dimensional imaging of the Costa Rica accretionary prism: Structural diversity in a small volume of the lower slope. *Journal of Geophysical Research,* **97**, 4439–4459.

Sibuet, J.-C. & Hsu, S.-K. 1997. Geodynamics of the Taiwan arc –arc collision. *Tectonophysics,* **274,** , 221–251.

Song, S.-R. & Lo, H.-J. 2002. Lithofacies of volcanic rocks in the central Coastal Range, eastern Taiwan; implications for island arc evolution. *Journal of Asian Earth Sciences,* **21**, 23-38.

Stein, M. & Hofmann, A. W. 1994. Mantle plumes and episodic crustal growth. *Nature,* **372**, 63–68.

Stern, C. R. 2004. Active Andean volcanism: its geologic and tectonic setting. *Revista Geologica de Chile,* **31**, 161–206.

Stern, R. J. & Bloomer, S. H. 1992. Subduction zone infancy: examples from the Eocene Izu-Bonin-Mariana and Jurassic California arcs. . *Geological Society of America Bulletin,* **104**, 1621–1636.

Suppe, J. 1981. Mechanics of mountain building and metamorphism in Taiwan. Geological Society of China, Memoir, 4, pp. 67–89.

Suppe, J. 1984. Kinematics of arc-continent collision, flipping of subduction, and backarc spreading near Taiwan. In *A special volume dedicated to Chun-Sun Ho on the occasion of his retirement.* (Ed, S. F. Tsan), Geological Society of China Memoir, 6, pp. 21–33.

Suyehiro, K., Takahashi, N., Ariie, Y., Yokoi, Y., Hino, R., Shinohara, M., Kanazawa, T., Hirata, N., Tokuyama, H. & Taira, A. 1996. Continental crust, crustal underplating, and low-Q upper mantle beneath an oceanic island arc. *Science,* **272**, 390-392.

Taylor, S. R. & McLennan, S. M. 1995. The geochemical evolution of the continental crust. *Reviews of Geophysics,* **33**, 241–265.

Teng, L. S. 1990. Geotectonic evolution of late Cenozoic arc-continent collision in Taiwan. *Tectonophysics,* **183**, 57–76.

Teng, L. S. 1996. Extensional collapse of the northern Taiwan mountain belt. *Geology,* **24**, 949–952.

Teng, L. S., Lee, C.-T., Tsai, Y.-B. & Hsiao, L.-Y. 2000. Slab breakoff as a mechanism for flipping of subduction polarity in Taiwan. *Geology,* **28**, 155–158.

Treloar, P. J., Petterson, M. G., Jan, M. Q. & Sullivan, M. A. 1996. A re-evaluation of the stratigraphy and evolution of the Kohistan arc sequence, Pakistan Himalaya: Implications for magmatic and tectonic arc-building processes. *Journal of the Geological Society,* **153**, 681-693.

Tsao, S. H., Li, T.-C., Tien, J.-L., Chen, C.-H., Liu, T.-K. & Chen, C.-H. 1992. Illite crystallinity and fission track ages along the east central cross-island highway of Taiwan. *Acta Geologica Taiwanica,* **30**, 45-64.

Tsuchi, R. 1992. Neogene events in Japan and on the Pacific coast of South America. *Revista Geologica de Chile,* **19**, 67–73.

Valentine, R. B., Morris, J. D., Duncan, D., Jr. & ODP Scientific Party Leg 170 1997. Sediment subduction, accretion, underplating and arc volcanism along the margin of Costa Rica: Constraints from Ba, Zn, Ni, and 10Be concentrations. *Eos, Transactions, American Geophysical Union,* **78**, 673.

Vannucchi, P., Scholl, D. W., Meschede, M. & McDougall-Reid, K. 2001. Tectonic erosion and consequent collapse of the Pacific margin of Costa Rica: Combined implications from ODP Leg 170, seismic offshore data, and regional geology of the Nicoya Peninsula. *Tectonics,* **20**(5), 649-668.

Vannucchi, P., Ranero, C. R., Galeotti, S., Straub, S. M., Scholl, D. W. & McDougall-Ried, K. 2003. Fast rates of subduction erosion along the Costa Rica Pacific margin: Implications for nonsteady rates of crustal recycling at subduction zones. *Journal of Geophysical Research-Solid Earth,* **108, 2511**(B11), doi:10.1029/2002JB002207.

Vannucchi, P., Galeotti, S., Clift, P. D., Ranero, C. R. & von Huene, R. 2004. Long-term subduction-erosion along the Guatemalan margin of the Middle America Trench. *Geology,* **32**(7), 617-620.

Vannucchi, P., Remitti, F. & Bettelli, G. 2008. Geological record of fluid flow and seismogenesis along an erosive subducting plate boundary. *Nature,* **451**, 699-704, doi:10.1038/nature06486.

Vita-Finzi, C. & Lin, J. C. 1998. Serial reverse and strike slip on imbricate faults: The Coastal Range of east Taiwan. *Geology,* **26**, 279–282.

von Huene, R., Langseth, M., Nasu, N. & Okada, H. 1982. A summary of Cenozoic tectonic history along the IPOD Japan trench transect. *Geological Society of America Bulletin,* **93**, 829–846.

von Huene, R. & Lee, H. 1982. The possible significance of pore fluid pressures in subduction zones. In *Studies in Continental Margin Geology.* (Eds, J. S. Watkins and C. L. Drake): American Association of Petroleum Geologists, Memoir, 34, pp. 781–791.

von Huene, R. & Scholl, D. W. 1991. Observations at Convergent Margins Concerning Sediment Subduction, Subduction Erosion, and the Growth of Continental-Crust. *Reviews of Geophysics,* **29**(3), 279-316.

von Huene, R. & Ranero, C. R. 2003. Subduction erosion and basal friction along the sediment-starved convergent margin off Antofagasta, Chile. *Journal of Geophysical Research,* **108, 2079**(B2), doi:10.1029/2001JB001569.

von Huene, R., Ranero, C. & Vannucchi, P. 2004. Generic model of subduction erosion. *Geology,* **32**, 913–916.

Wang, T.-K., Lin, S.-F., Liu, C.-S. & Wang, C.-S. 2004. Crustal structure of southernmost Ryukyu subduction zone; OBS, MCS and gravity modelling. *Geophysical Journal International,* **157**, 147–163.

Wells, R. E., Blakely, R. J., Sugiyama, Y., Scholl, D. W. & Dinterman, P. A. 2003. Basin-centered asperities in great subduction zone earthquakes: A link between slip, subsidence, and subduction erosion? *Journal of Geophysical Research,* **108**(B10), doi:10.1029/2002JB002072.

Willett, S., Beaumont, C. & Fullsack, P. 1993. Mechanical model for the tectonics of doubly vergent compressional orogens. *Geology,* **21**, 371–374.

Willett, S. D., Fisher, D., Fuller, C., Chao, Y.-E. & Yu, L.-C. 2003. Erosion rates and orogenic-wedge kinematics in Taiwan inferred from fission-track thermochronometry. *Geology,* **31**(11), 945-948.

Wise, D. U. 1974. Continental margins, freeboard and the volumes of continents and oceans through time. In *The Geology of Continental Margins.* (Eds, C. A. Burk and C. L. Drake), New York: Springer-Verlag, pp. 45–58.

Zhang, P., Molnar, P. & Downs, W. R. 2001. Increased sedimentation rates and grain sizes 2–4 Myr ago due to the influence of climate change on erosion rates. *Nature,* **410**, 891–897.

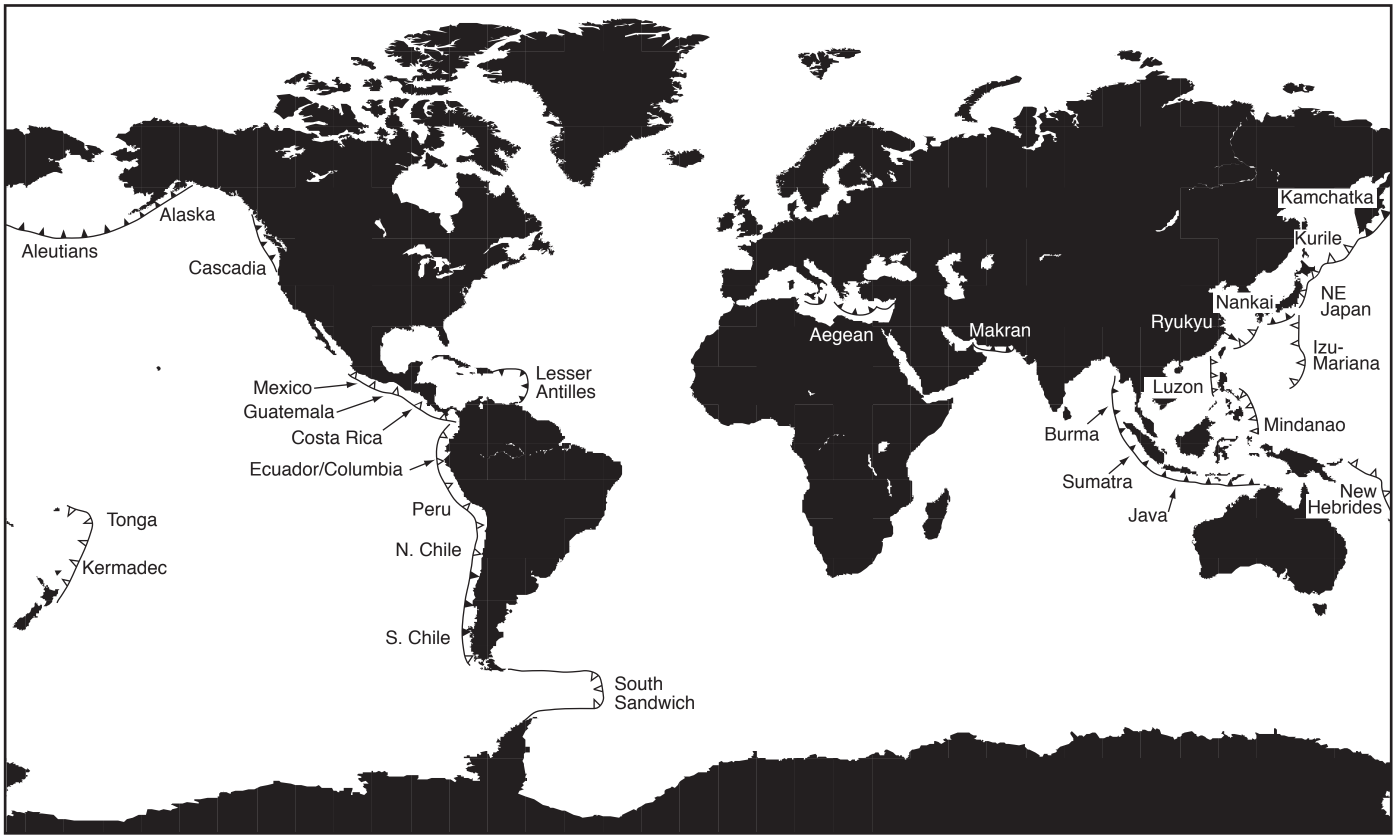

Figure 1
Clift et al.

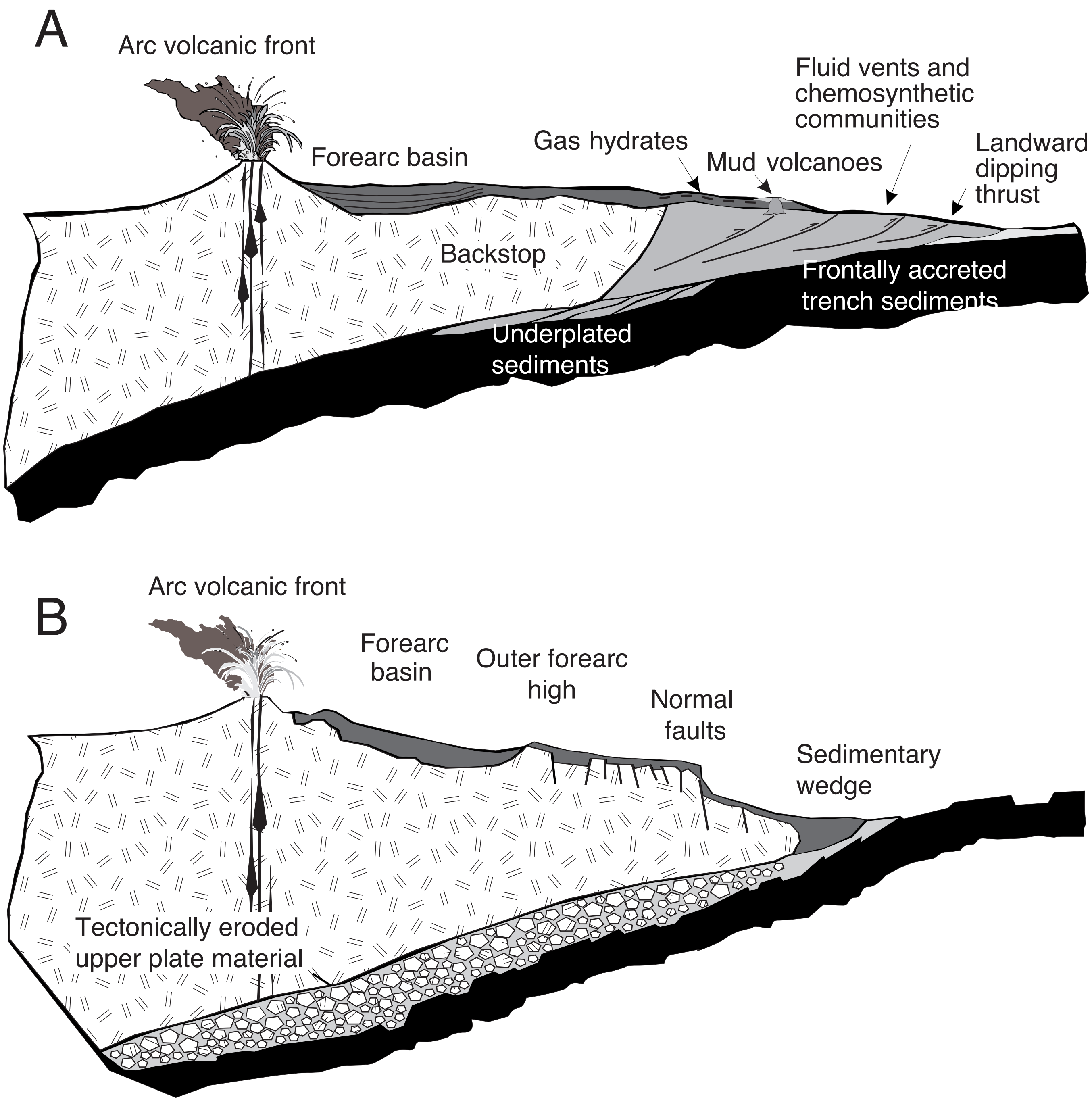

Figure 2
Clift et al.

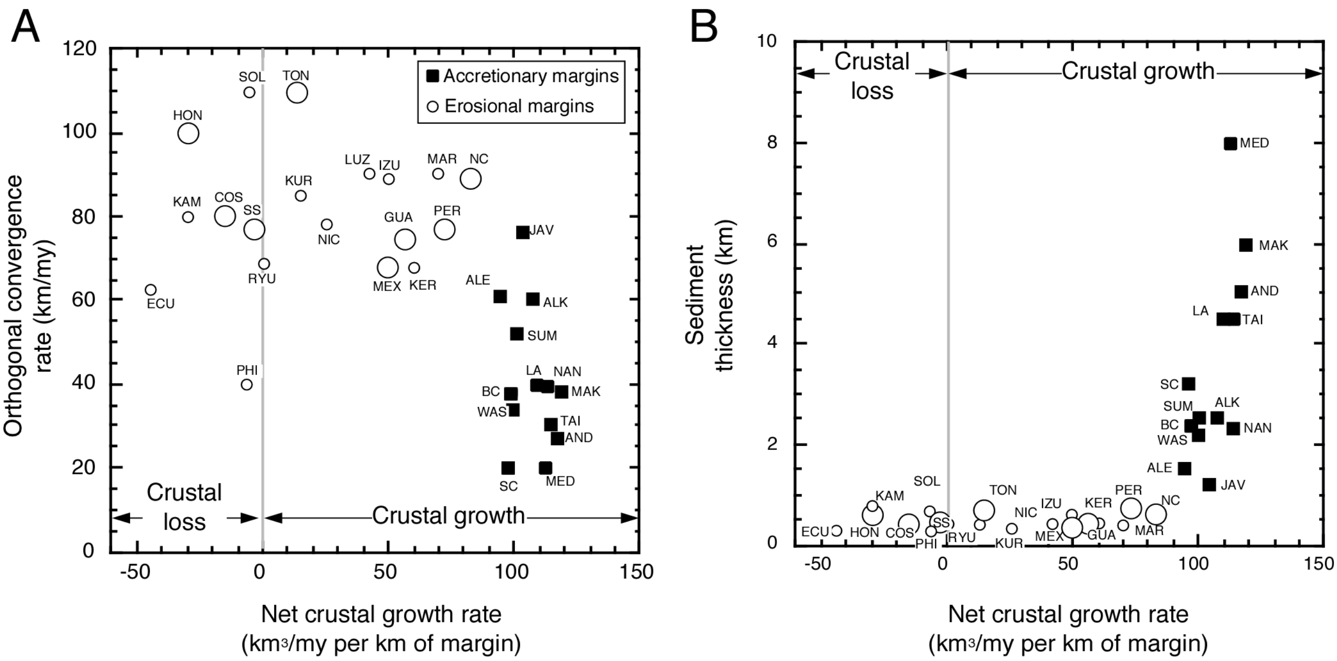

Figure 3
Clift et al.

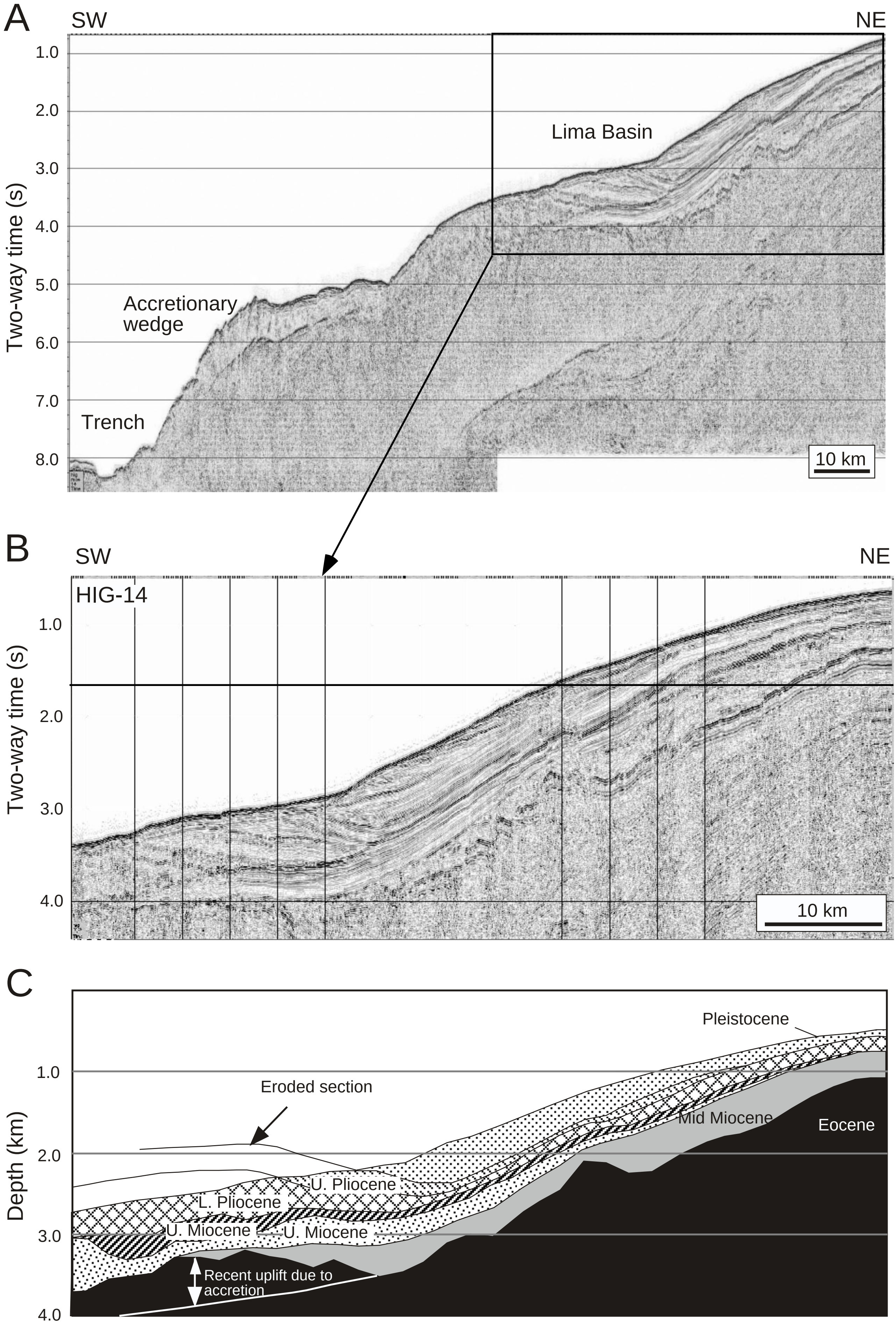

Figure 4
Clift et al.

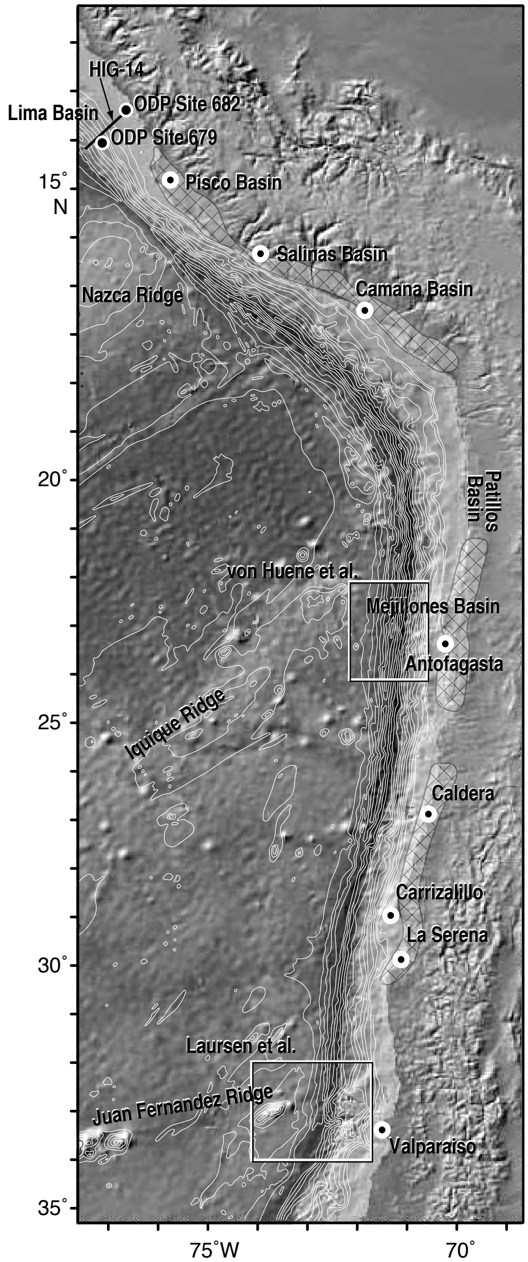

Figure 5
Clift et al.

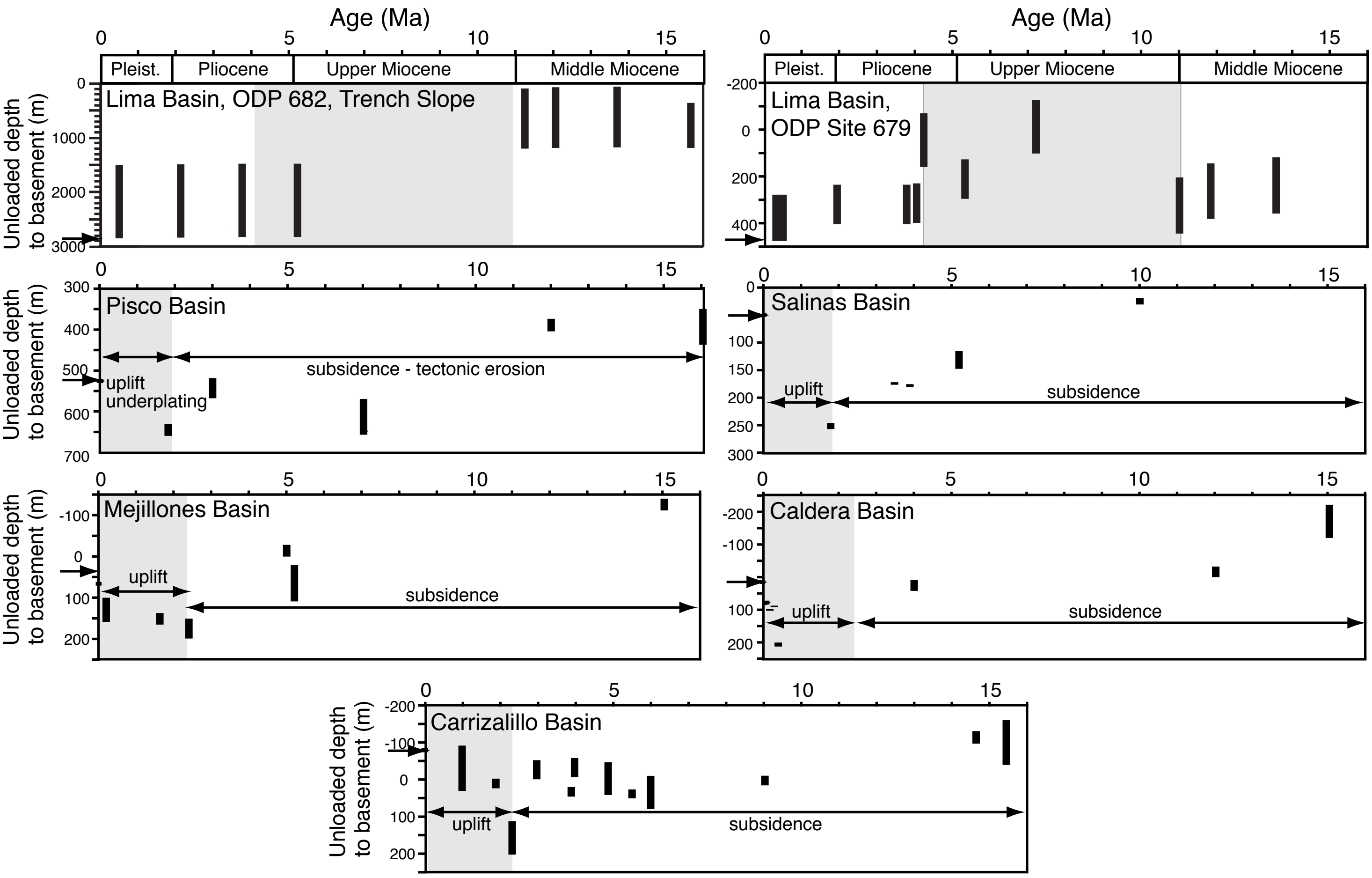

Figure 6
Clift et al.

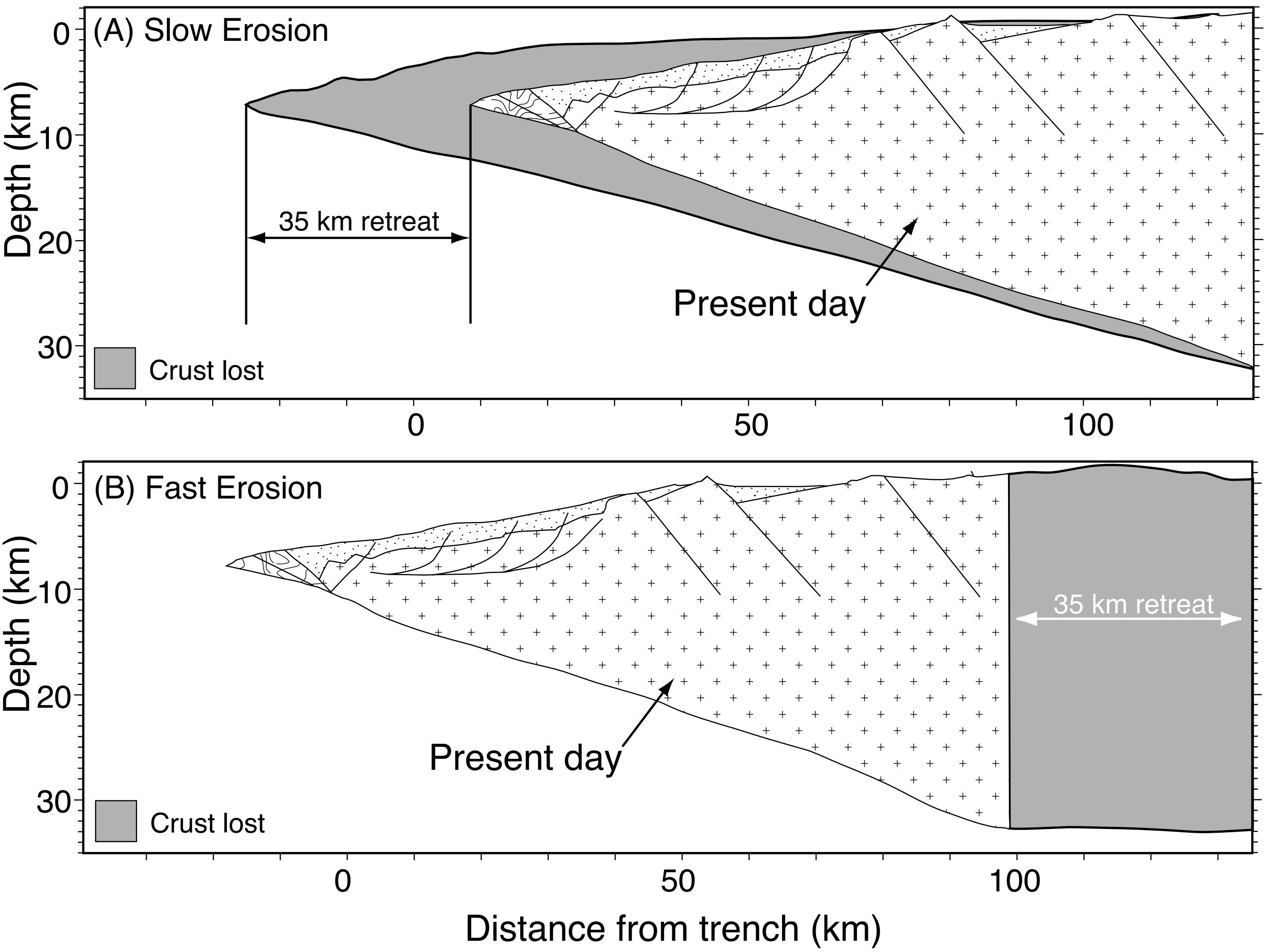

Figure 7
Clift et al.

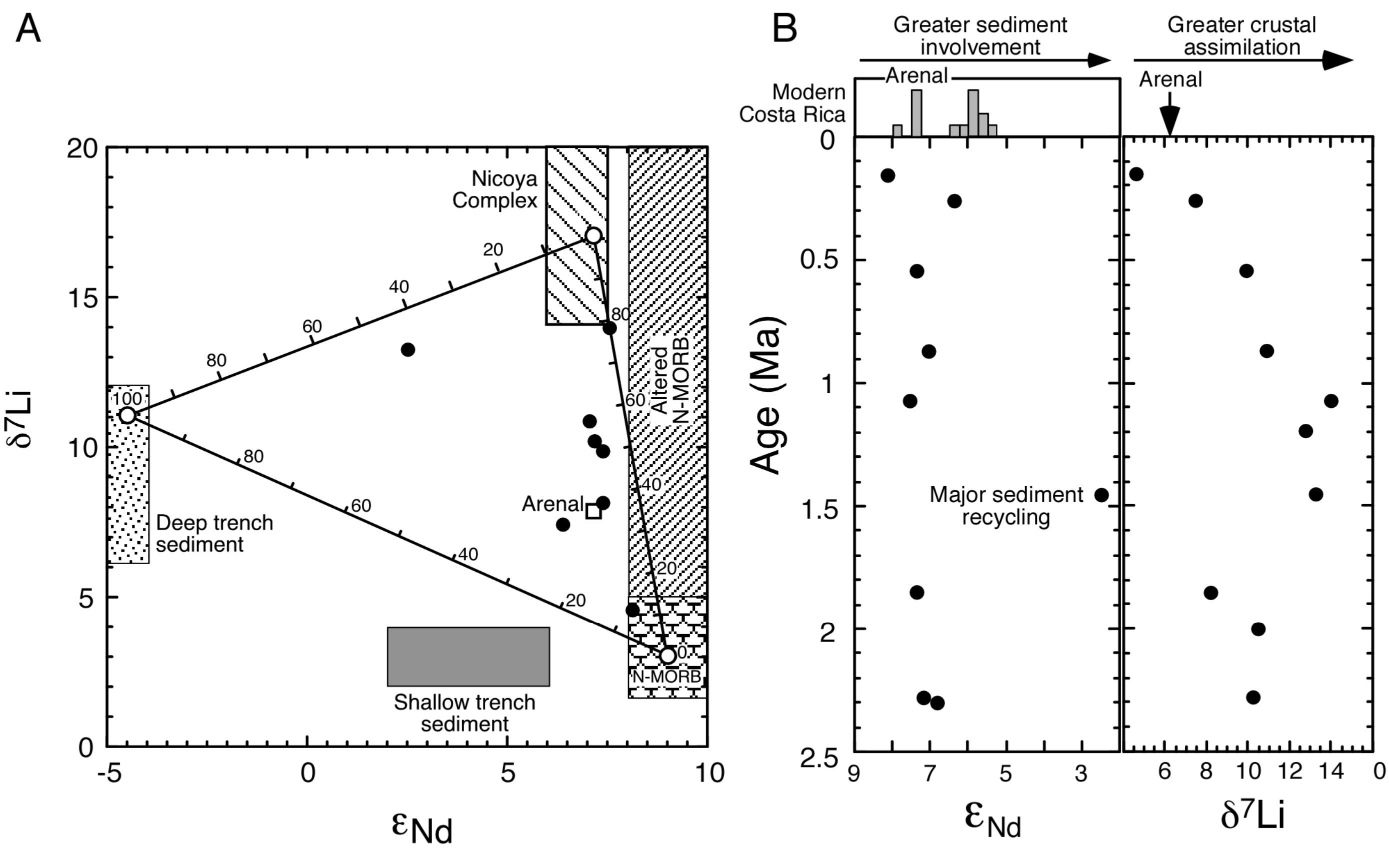

Figure 8
Clift et al.

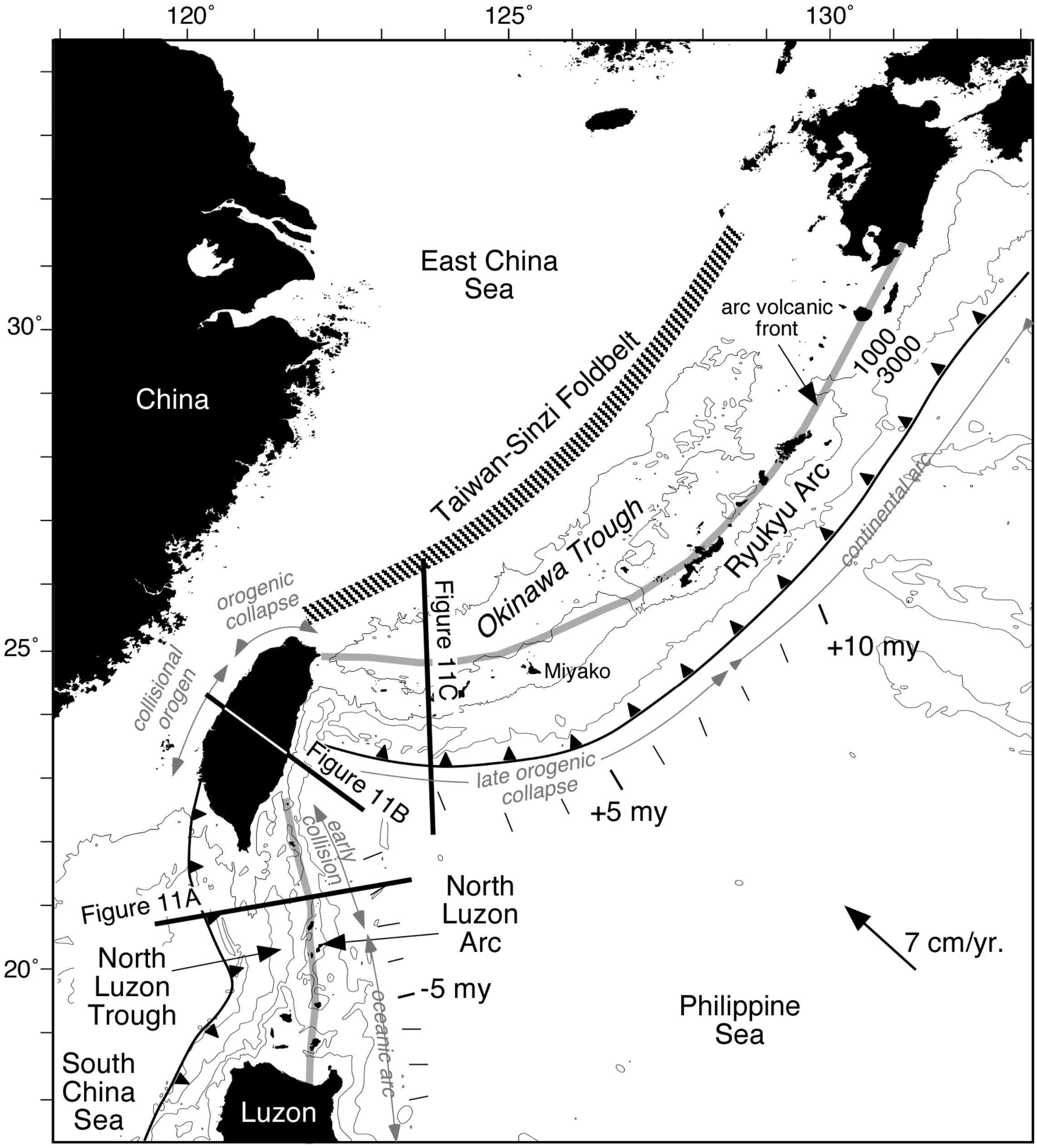

Figure 9
Clift et al.

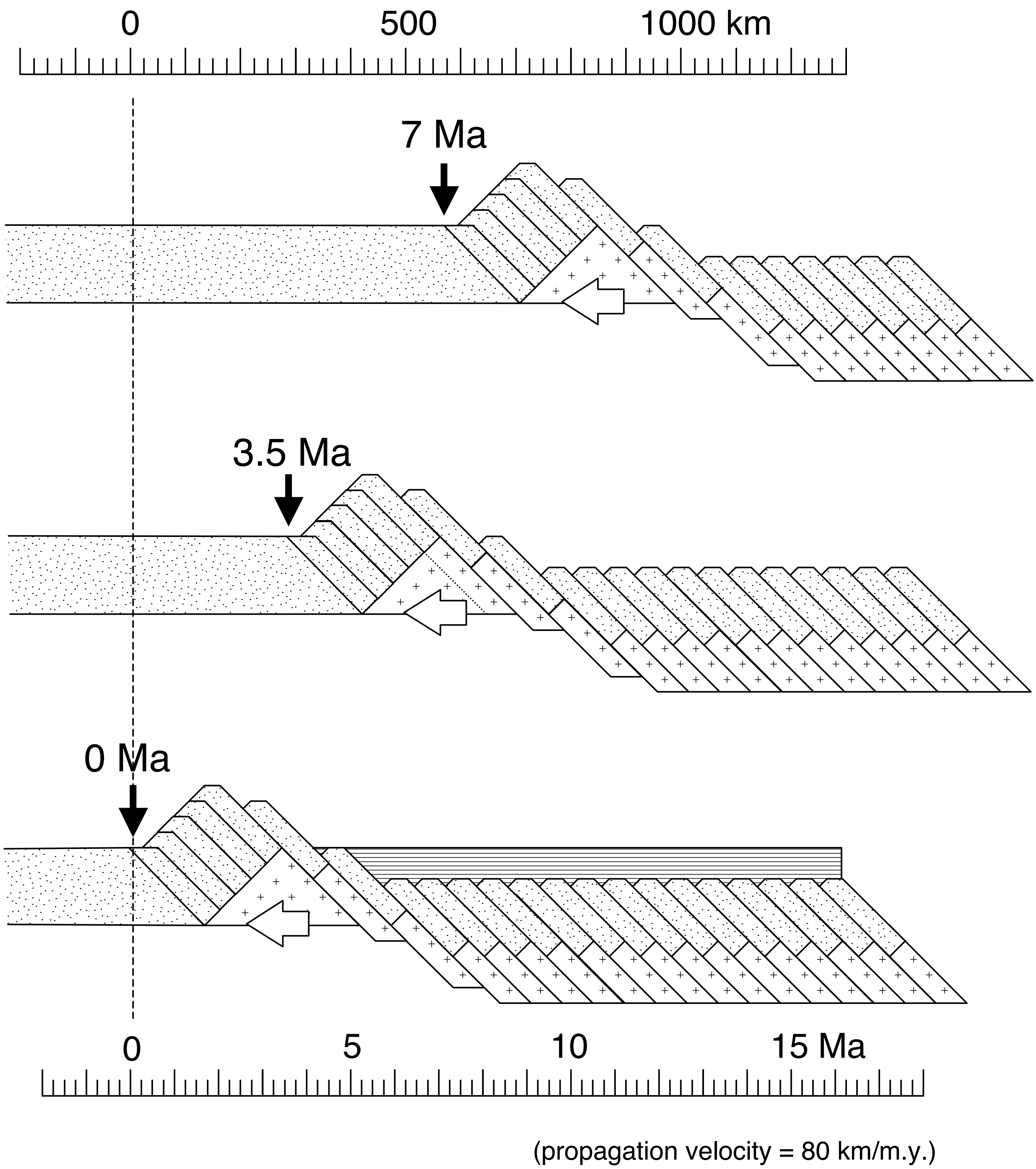

Figure 10
Clift et al.

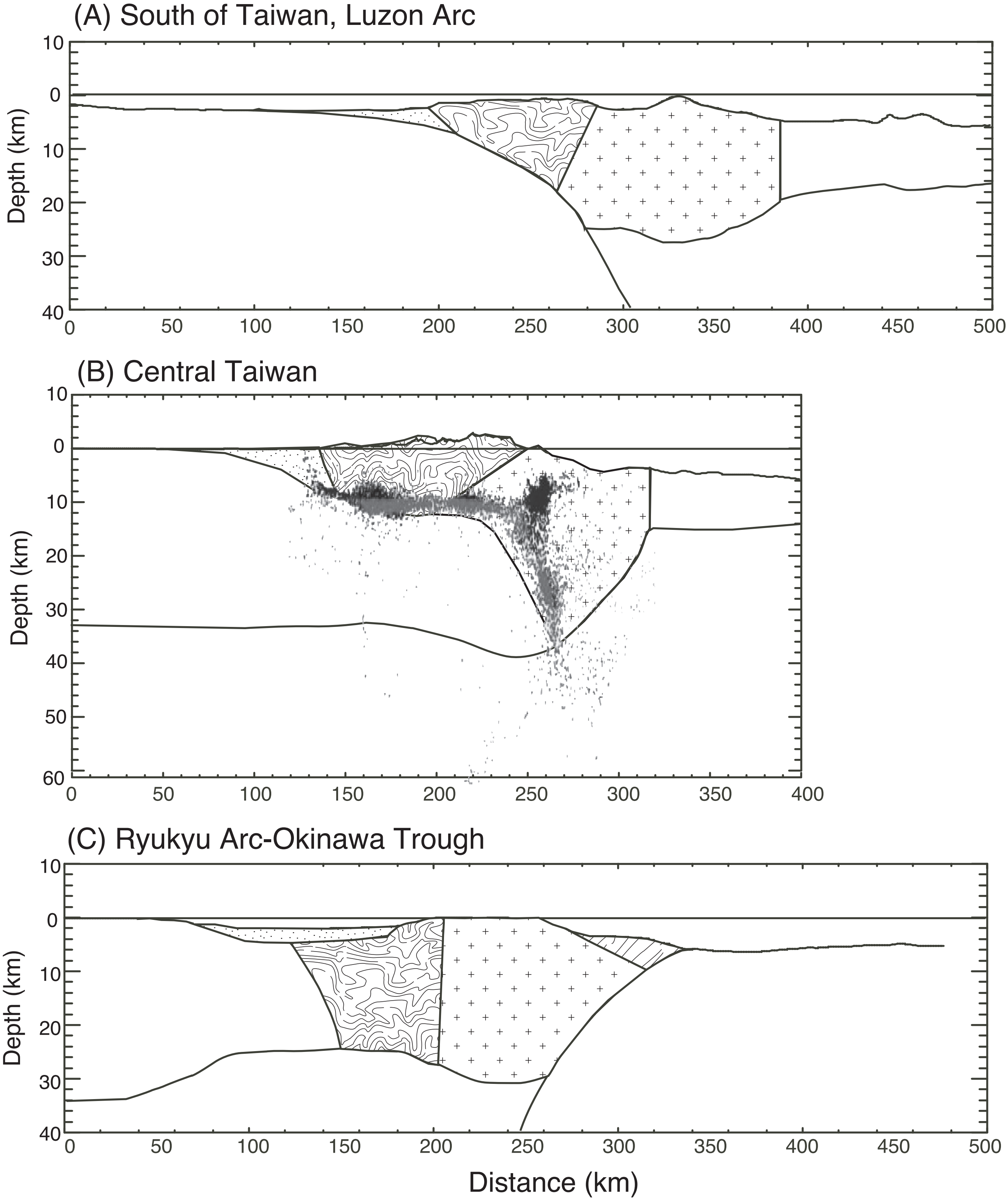

Figure 11
Clift et al.

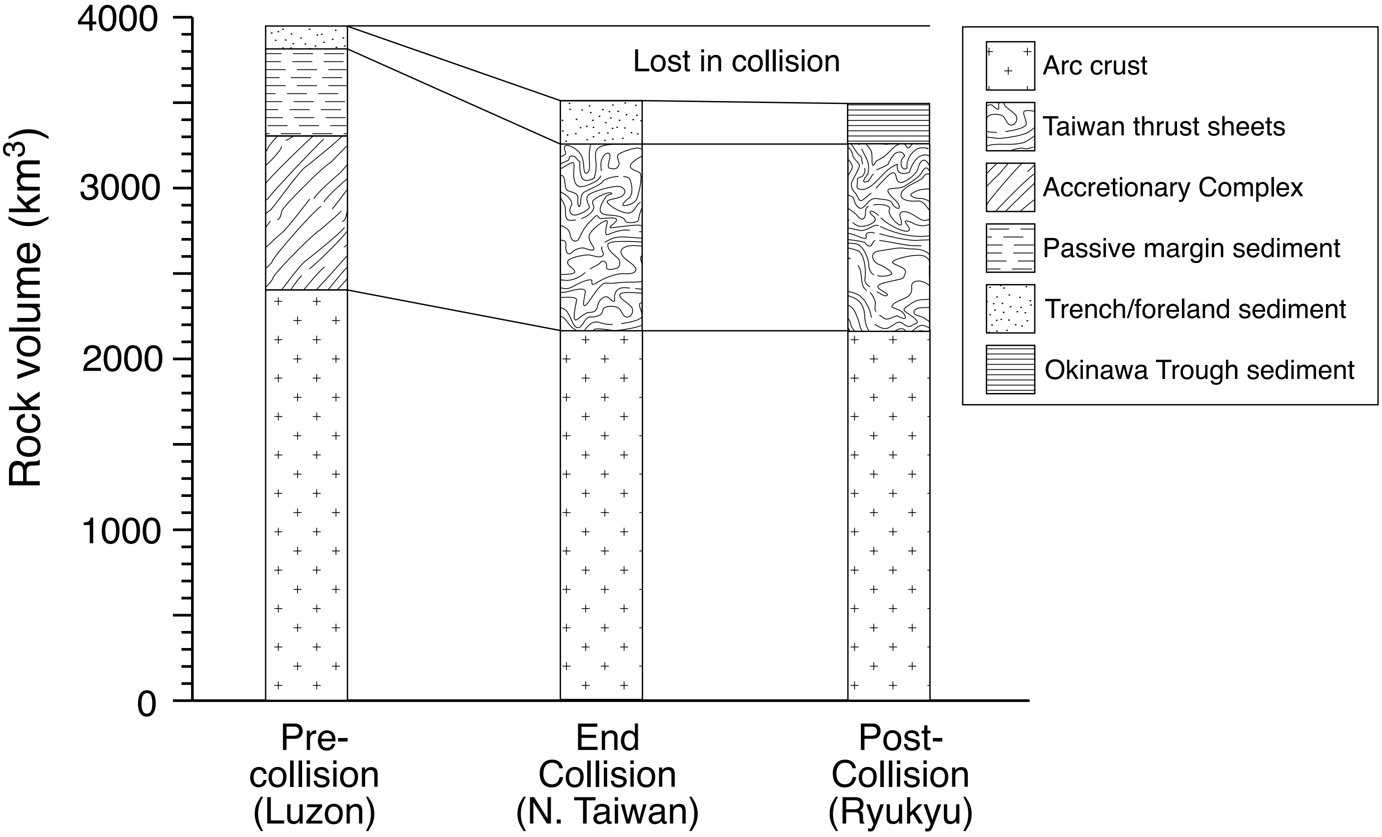

Figure 12
Clift et al.

(A)

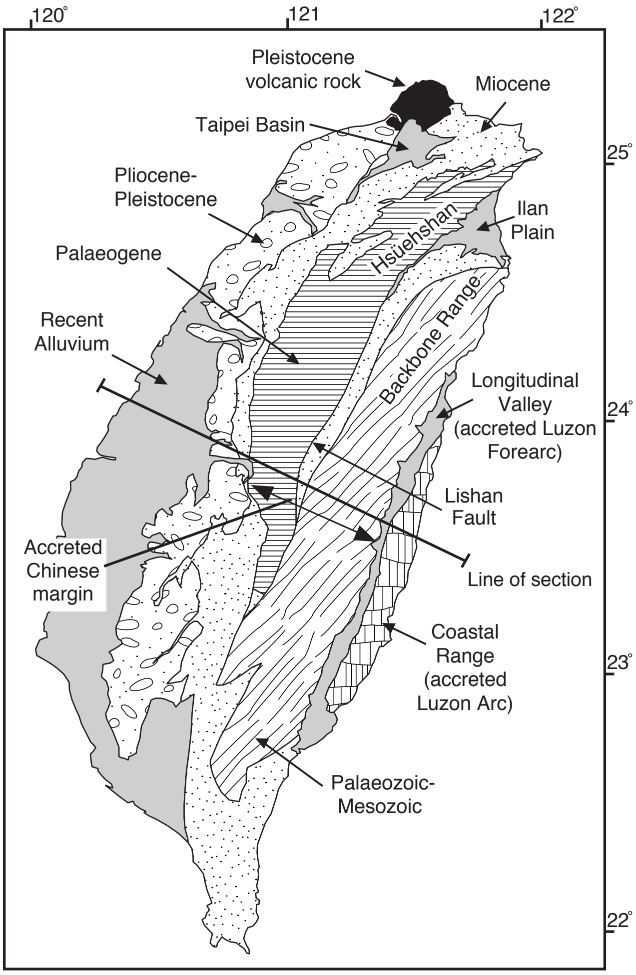

(B)

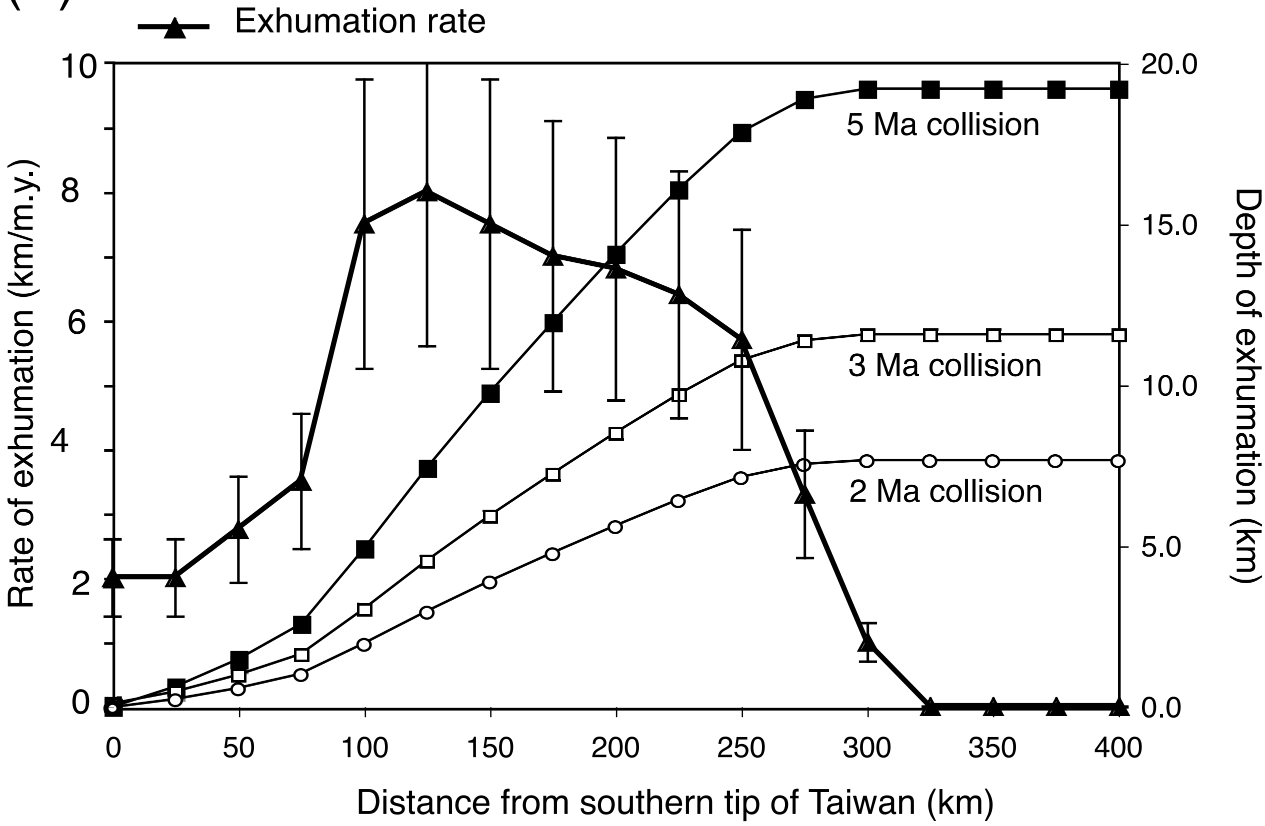

Figure 13
Clift et al.

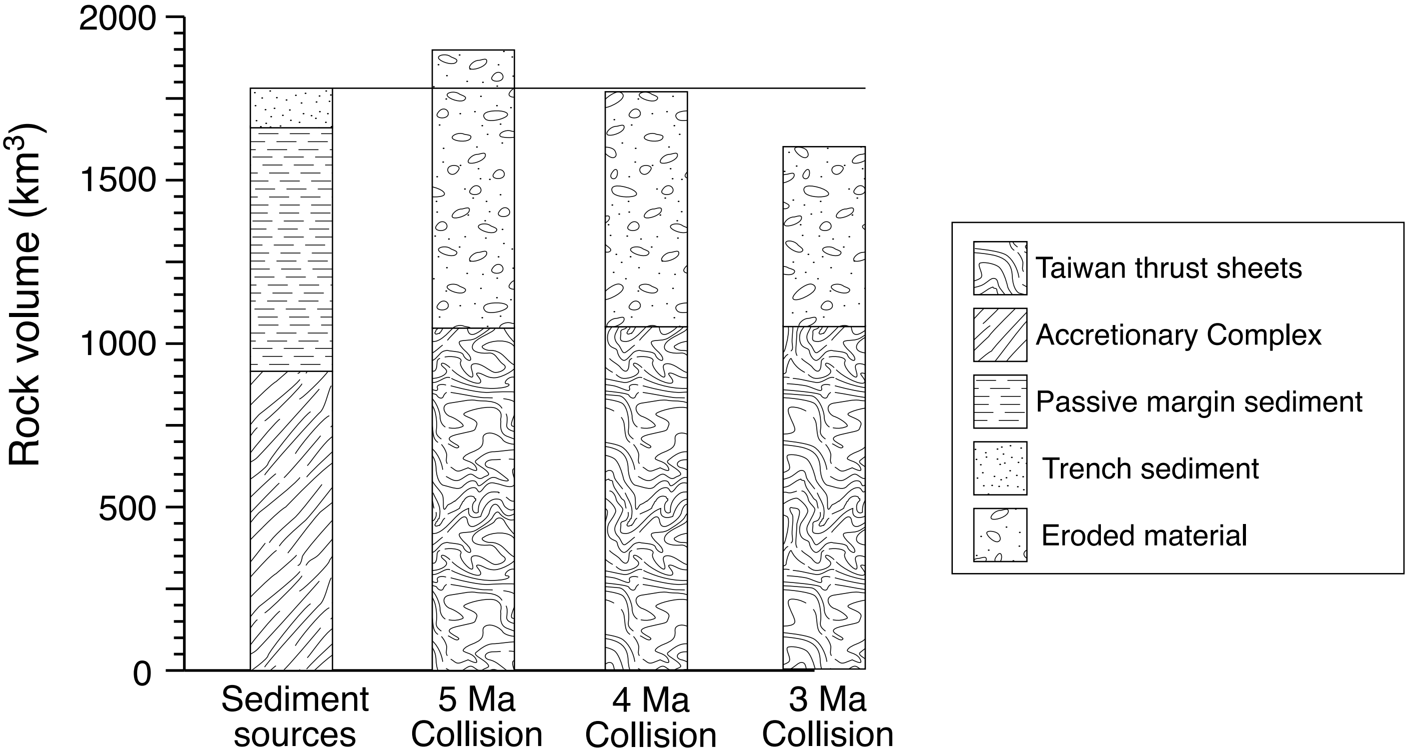

Figure 14
Clift et al.

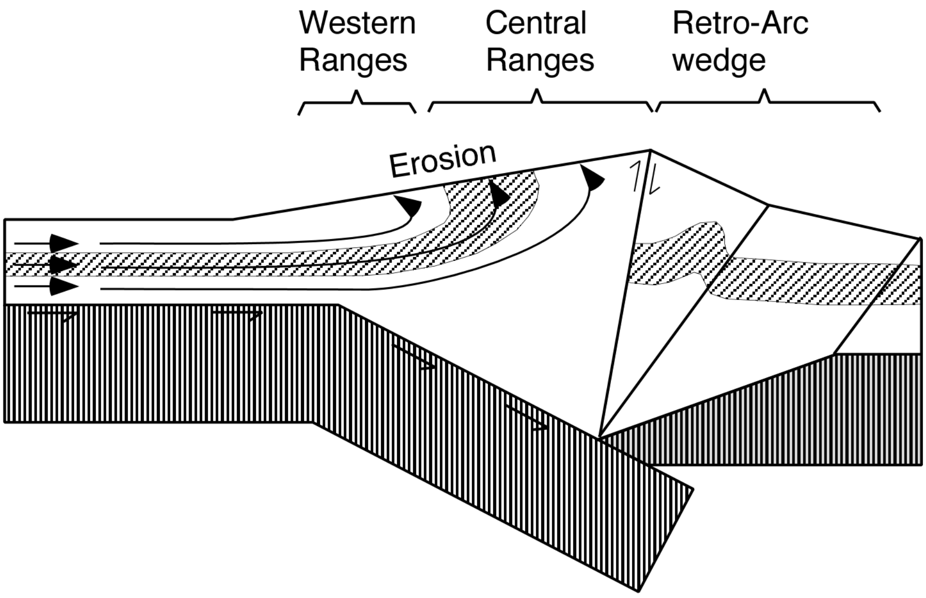

Figure 15
Clift et al.

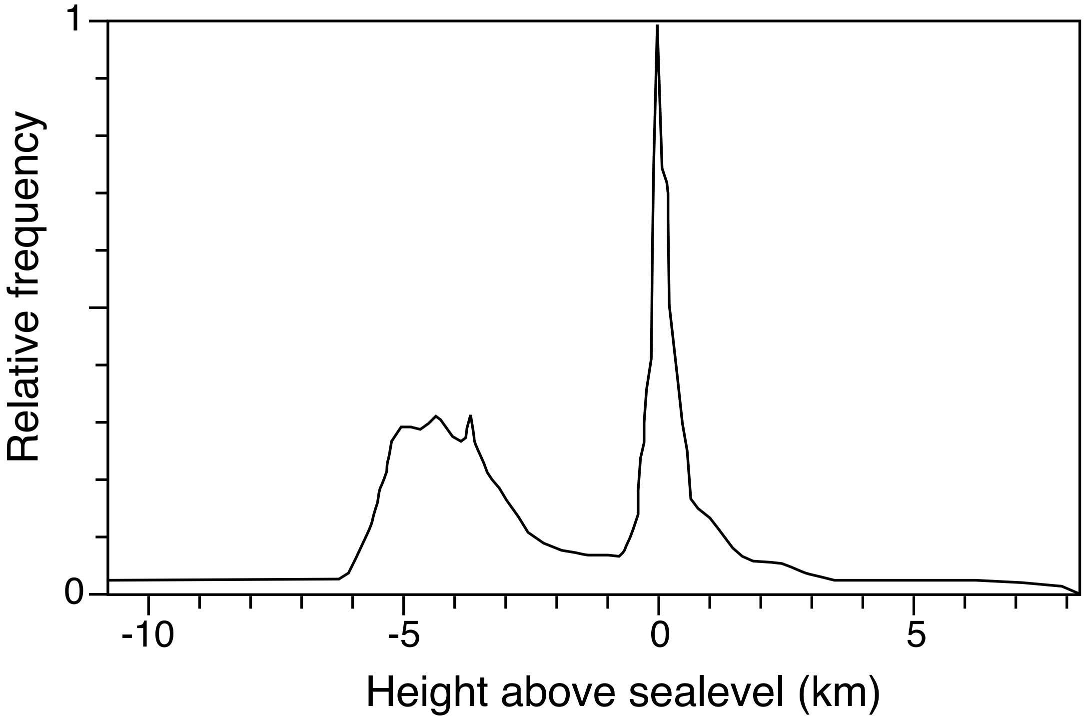

Figure 16
Clift et al.

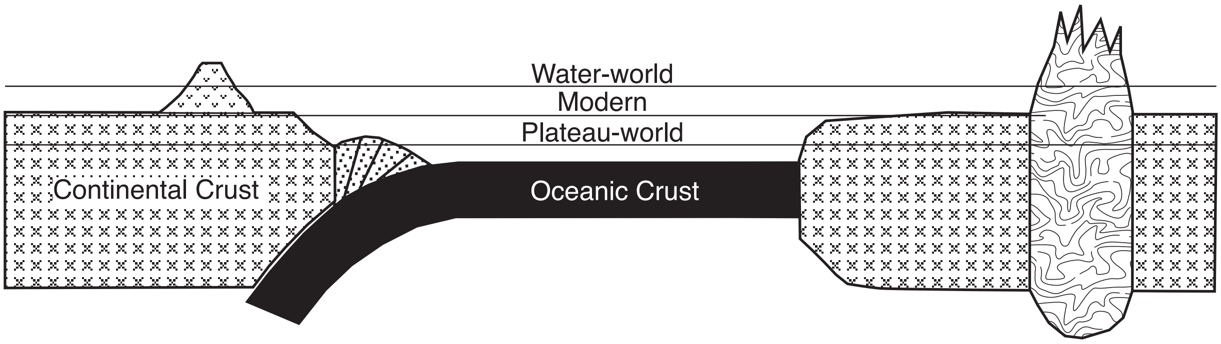

Figure 17
Clift et al.

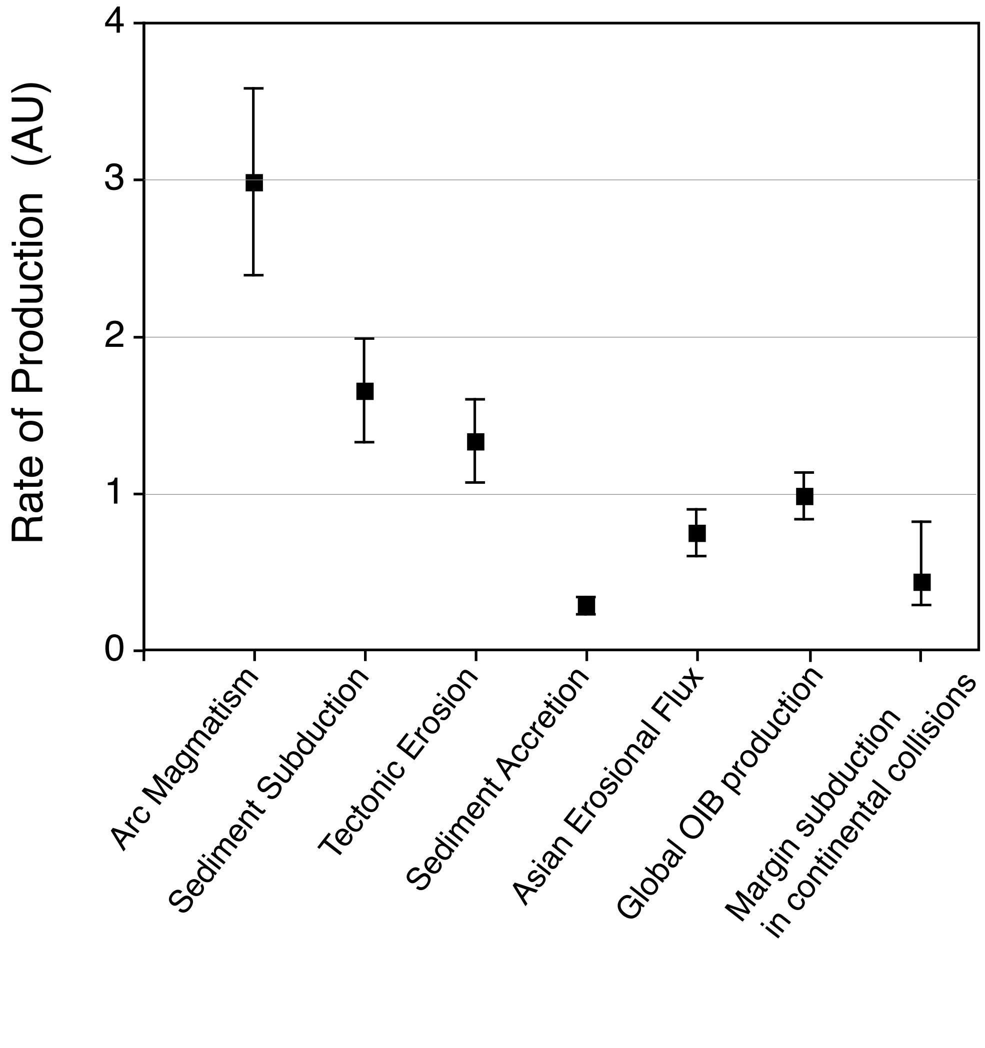

Figure 18
Clift et al.

Table 1

Cenozoic Orogen	**Length of subducted margin (km)**
Alboran Sea	1300
Pyrenees	450
Alps-Appennines-Hellenides	3000
Turkey-Zagros	3100
Himalaya	2700
Taiwan-Ryukyu	1100
Borneo	1300
Australia-Papua New Guinea	2800
Total	**15750**

Margin type	**% of total**	**Length of margin (km)**	**Width of COT (km)**	**Average crustal thickness (km)**	**Volume (km^3)**
Volcanic	50	7875	50	18	7087500
Non-volcanic	50	7875	150	18	21262500
Total					**28350000**

Table 2

Arc	Length (km)	Orthogonal rate of convergence (km/my)	Trench retreat rate (km/my)	Trench sediment thickness (km)	Rate of sediment delivery (km^3/m.y./km)	Rate of forearc erosion (km^3/m.y./km)	Rate of sediment accretion (km^3/m.y./km)	Rate of crustal subduction (km^3/m.y./km)	Efficiency of sediment accretion (%)	Magmatic Productivity Rate (km^3/m.y./km)	Net crustal growth rate (km^3/m.y./km)
Erosive Margins											
North Chile	2000	89	3.0	0.3	13	15		28		99	84
Peru	2200	77	3.1	0.7	29	15		44		86	71
Ecuador-Colombia	1100	63	3.0	0.6	20	15		35		71	56
Costa Rica	450	80	3.0	0.4	17	105		122		89	-16
Nicaragua	275	78	2.0	0.3	12	64		76		86	22
Guatemala	500	74	0.9	0.3	12	34		46		82	48
Mexico	1700	68	1.0	0.6	22	40		62		75	35
Kurile	1100	85	3.0	0.5	20	75		95		94	19
Kamchatka	1100	80	3.0	0.8	36	120		156		89	-31
NE Japan	1000	100	3.0	0.8	45	120		165		111	-9
Mariana	1600	90	1.0	0.4	19	20		39		100	80
Izu-Bonin	1300	89	2.0	0.4	19	40		59		99	59
Ryukyu	1000	69	3.0	0.4	14	90		104		77	-13
South Luzon	400	90	1.5	0.4	19	48		67		100	52
Philippine	1000	40	3.0	0.6	13	96		109		45	-51
Tonga	1500	110	3.8	0.4	23	76		99		122	46
Kermadec	1250	68	1.5	0.4	14	30		44		75	45
Solomons	2750	110	3.8	0.3	17	95		112		122	27
South Sandwich	700	77	4.7	0.4	16	94		110		86	-8
Accretionary Margins											
South Chile	2000	20		3.2	43		7	36	16	22	29
Lesser Antilles	850	40		4.5	137		19	118	14	44	64
Oregon-Washington	850	34		2.2	48		10	38	21	38	48
British Columbia	550	38		2.5	61		10	51	16	42	52
Aleutians	1500	61		1.5	54		4	50	7	68	72
Alaska	2050	60		2.5	96		17	79	18	67	84
Taiwan-North Luzon	700	30		4.5	95		25	70	26	33	58
SW Japan-Nankai	900	39		2.3	65		24	41	37	44	68
Sumatra	1800	52		2.5	83		11	72	13	58	69
Java	2100	76		1.2	54		14	40	26	84	98
Burma-Andaman	1800	27		5.0	99		27	71	28	31	58
Makran	1000	38		6.0	179		29	150	16	42	71
Aegean	1200	20		8.0	131		22	109	17	22	45

Table 3

	Rate (AU)
Arc magma production	2.98
Sediment subduction	1.65
Tectonic erosion	1.33
Subduction accretion	0.28
Total river discharge	6.70
Mainland Asian erosion	0.75
MORB production	20.00
OIB Production	0.5
Subduction of passive margins in orogens	0.4

Table 4

Tectonic Unit	Volume (km^3/km of trench)
Taiwan thrust sheets	1076
Sediment in Taiwan foreland	250
Trench sediment in Luzon Trench	125
Accretionary prism offshore Luzon	825
Arc under Taiwan	2155
Luzon Arc igneous crust	2475
Ryukyu accretionary prism	210
Sediment in Okinawa Trough	300
Sediment on S China margin	750
Sediment eroded from Taiwan (5 Ma collision)	880
Sediment eroded from Taiwan (4 Ma collision)	720
Sediment eroded from Taiwan (3 Ma collision)	550

Table 5

Basin	**Eroded rock volume (km^3)**	**Percentage of total**
Bengal Fan	10271159	36.8
Indus Fan	4108463	14.7
Sediment subducted in Andaman Trench	3200000	11.5
Himalayan Foreland Basin	2042711	7.3
Central Asian Basins (Tarim, Junggar,	1900000	6.8
Irrawaddy Fan	1472473	5.3
Sediment subducted in Makran	1300000	4.7
Song Hong/Yinggehai Basin	451931	1.6
Katawaz Basin	389972	1.4
Sulaiman/Kirthar Ranges	389972	1.4
East China Sea	345111	1.2
Pearl River Mouth Basin	328677	1.2
Malay Basin	315530	1.1
Nam Con Son Basin	287592	1.0
SE Hainan Basin (Qiongdongnan Basin)	246508	0.9
Burma Basin	237697	0.9
Mekong/Cuu Long Basin	177486	0.6
Indo-Burma Ranges	129991	0.5
Bohai Gulf	123254	0.4
Pengyu Basin	65735	0.2
Pattani Trough	65078	0.2
West Natuna Basin	36976	0.1
Hanoi Basin	8124	0.0
Total eroded	**27894442**	

Table 6

	Rate of Erosion (km^3/m.y.)	Armstrong Units
Average erosion rate since 50 Ma	557889	0.56
Average erosion rate since 33 Ma	845286	0.85
Average erosion rate since 22 Ma	1267929	1.27
Time required to erode modern Tibet at 50 Ma rate	220	
Time required to erode modern Tibet at 33 Ma rate	145	
Time required to erode modern Tibet at 22 Ma rate	97	